Copy 740

NASA TM X-492

TECHNICAL MEMORANDUM

X-492

Declassified by authority of NASA
Classification Change Notices No. 143
Dated ** 2-14-69

A RAPID METHOD OF ESTIMATING LAUNCHER SETTING TO CORRECT FOR THE EFFECTS OF WIND ON THE TRAJECTORY OF AN UNGUIDED FIN-STABILIZED ROCKET VEHICLE

By James T. Rose and Rodney G. Rose

Space Task Group
Langley Field, Va.

NATIONAL AERONAUTICS AND SPACE ADMINISTRATION
WASHINGTON
March 1961

DECLASSIFIED

CONFIDENTIAL

NATIONAL AERONAUTICS AND SPACE ADMINISTRATION

TECHNICAL MEMORANDUM X-492

A RAPID METHOD OF ESTIMATING LAUNCHER SETTING TO CORRECT FOR THE EFFECTS OF WIND ON THE TRAJECTORY OF AN UNGUIDED FIN-STABILIZED ROCKET VEHICLE*

By James T. Rose and Rodney G. Rose

SUMMARY

A method has been developed for estimating launcher settings to compensate for the effects of wind on the trajectory of Little Joe boosters used in a research and development program of Project Mercury. The necessity for correcting the effects of winds was brought about by a combination of characteristics inherent in the basic design of the Little Joe booster, low acceleration, a large amount of aerodynamic stability at take-off, and launchings at high elevation angles. This method of correcting for wind effects can be applied to all symmetrical fin-stabilized rocket vehicles having aerodynamic, performance, and inertia characteristics similar to those of the Little Joe booster vehicle.

A study of wind effects on the flight of a typical Little Joe vehicle, using a variety of wind profiles, was conducted using six-degree-of-freedom equations of motion in a trajectory simulation program. The results of these studies established the concepts and procedures used in the method of correction for wind effects. These principles involve a wind-effects investigation (for the specific vehicle being flight tested) using a set of constant wind-velocity profiles, a graphic presentation of the results of this investigation in carpet form, a determination of an average weighted wind velocity and direction to represent the measured wind profile near the time of launch and over the altitude range in which winds are assumed to affect the trajectory of the vehicle, and an application of this average weighted wind velocity and direction to the carpet plots in order to determine the corrections to be applied to the nominal launcher setting.

*Title, Unclassified.

[redacted]

This method of estimating launcher settings to compensate for the effects of wind has been used for four Little Joe launchings and has resulted in deviations from desired conditions as follows: azimuth angles, 4.0°, 2.0°, 1.5°, and 2.0° and elevation angles 0.4°, 0.4°, 1.9°, and 0.3°, respectively. The calculated correction angles were as follows: azimuth angles, 16°, 24°, 17°, and 0° and elevation angles, 2.0°, 1.0°, 4.0°, and 7.0°, respectively.

INTRODUCTION

In order to make a fin-stabilized, unguided rocket vehicle fly on a prescribed trajectory, launcher corrections must be applied to compensate for deviations in the azimuth and elevation planes produced by wind effects. An expedient yet accurate method of correcting for wind effects, which permits final wind readings and correction calculations shortly before launch, is required to minimize the chance of error in the final corrected launcher setting.

A method of correcting a launcher setting for wind effects which makes it possible to use the measured wind data recorded just prior to launch has been developed. This method of correcting for wind effects gives initial heading and elevation angles for the vehicle, but makes no allowance for drift due to the wind effects. In actual practice, for this type of vehicle, the difference between course and track due to this drift effect is negligible.

This method of correcting launcher settings for wind effects is a method that can be applied to all vehicles having aerodynamic, performance, and inertia characteristics similar to those of the Little Joe.

SYMBOLS

C_D drag coefficient

C_L lift coefficient

C_m pitching-moment coefficient

d_e nozzle exit diameter, in.

d_t nozzle throat diameter, in.

UNCLASSIFIED

F	axial thrust, lb
$\bar{F}$	average thrust, lb
G	average gradient of wind-velocity profile, $\frac{\text{ft/sec}}{\text{1,000 ft}}$
g	acceleration due to gravity, ft/sec^2
h	altitude, ft
I_{sp}	specific impulse, $\frac{\text{lb-sec}}{\text{lb}}$
M	Mach number
m	any integer
n	any integer
r	sensitivity factor for wind direction in azimuth plane
s	sensitivity factor for wind direction in elevation plane
T	temperature, ^{o}F
t	time, sec
t_b	time of web burnout, sec
t_f	time of final burnout, sec
V	wind velocity, ft/sec
$\bar{V}$	average wind velocity, ft/sec
$\bar{V}_w$	average weighted wind velocity, ft/sec
WF	weighting factor
α	angle of attack, deg
γ	elevation angle at launch, deg
γ_n	nominal or desired elevation angle at launch, deg
γ_c	elevation angle at launch with correction applied, deg
γ_t	flight-path angle at 10 seconds, deg

γ_{nt} nominal or desired flight-path angle at 10 seconds, deg

γ_{at} measured flight-path angle at 10 seconds, deg

γ_a elevation angle at launch which would give γ_{at} in no-wind condition, deg

$\Delta\gamma$ change in flight-path angle over any increment of altitude, deg

$\Delta\gamma_T$ total change in flight-path angle between ground and altitude of total wind effect, deg

θ_W angle from north from which wind is blowing, deg

Λ_n nominal or desired azimuth, deg

Λ_c launch azimuth with correction applied, deg

Λ_a measured flight azimuth, deg

ϕ correction angle in azimuth, deg

ψ angle between wind direction and longitudinal axis of rocket vehicle, measured from rear of vehicle, deg

ψ_{AW} angle between wind direction and desired azimuth of vehicle, deg

$\bar{\psi}_{AW}$ average angle over altitude increments between wind direction and desired azimuth of vehicle, deg

ψ_o angle between wind direction and vehicle at launch, deg

$\Delta\psi$ change in heading angle over any increment of altitude, deg

$\Delta\psi_T$ total change in heading angle between ground and altitude of total wind effect, deg

Subscripts

sl sea level

v vacuum

DECLASSIFIED

PERFORMANCE AND AERODYNAMIC CHARACTERISTICS OF THE LITTLE JOE VEHICLE

The general configuration of a typical Little Joe vehicle is shown in figure 1.

The booster propulsion system is composed of a cluster of six or eight solid-fuel rocket motors - two or four main and four auxiliary rocket motors. The main rocket motors can be either Thiokol Castor (XM-33E2) or Pollux (XM-33E4) rocket motors. The four auxiliary rocket motors are Thiokol Recruit motors (XM-19E1-C12). Figures 2, 3, and 4 show the typical thrust-time curves for Castor, Pollux, and Recruit rocket motors.

Several possibilities for combining these rocket motors exist. Some of these possibilities are:

(1) Four Recruit and four Castor

(2) Four Recruit and four Pollux

(3) Four Recruit and two Castor

(4) Four Recruit and two Pollux

For any combination of rocket motors, the nozzles are canted in order to direct the thrust vector of each rocket motor through the mean center-of-gravity position of the vehicle during the boosted phase of flight and thus to minimize destabilizing moments which would be generated in the event of a delay in the ignition of one or more of the motors.

If four auxiliary and four main rocket motors are combined, the sequence for igniting the rocket motors is four auxiliary and two main rocket motors (the first stage) at take-off with the remaining two main rocket motors (the second stage) being ignited at a predetermined time after take-off. If four auxiliary and only two main rocket motors are combined, all six rocket motors act as the first stage and are ignited at take-off.

Figure 5 is a calculated time history of altitude, velocity, and Mach number for a Little Joe flight test which used the combination of four Recruit and four Pollux rocket motors as the propulsion system. The two Pollux rocket motors of the second stage were ignited 25 seconds from take-off. For a flight test which used a combination of four Recruit rocket motors and two Pollux rocket motors as the propulsion system, a calculated time history of altitude, velocity, and Mach number is shown in figure 6.

Basically, the Little Joe vehicle is a fin-stabilized booster designed to be aerodynamically stable in the Mach number range between

0 and 6. Available wind-tunnel information is presented in tables I to IV and figure 7. The calculated moment of inertia in the pitch plane at take-off is approximately 80,000 slug-feet^2. Since the vehicle is symmetrical, the moment of inertia in the yaw plane is also 80,000 slug-feet^2. The moment of inertia in roll at take-off is approximately 6,600 slug-feet^2.

GENERAL STUDY OF WIND EFFECTS ON A LITTLE JOE VEHICLE

The Little Joe booster, because it is designed to be fin stabilized to Mach numbers to 6.0, has a high margin of aerodynamic stability at take-off.

On a fin-stabilized rocket vehicle, the magnitude of the wind effect on the prescribed flight trajectory increases with increasing aerodynamic stability of the vehicle and decreases with increasing take-off acceleration. Depending on the total weight and the number of rocket motors used on any proposed Little Joe flight test, the maximum take-off acceleration may vary from 6g to 10g. Studies, using a number of constant wind-velocity profiles from the ground to a 50,000-foot altitude orientated at various angles relative to the rocket vehicle, were made in order to determine the magnitude of the winds that affected the vehicle. Figure 8 is a sketch defining the various angles associated with the vehicle. A vehicle capable of a take-off acceleration of 6g was used for the studies since it represented the most serious condition. These theoretical studies were conducted with the use of six-degree-of-freedom trajectory simulation programs. The six-degree-of-freedom equations of motion used for the Little Joe studies are presented in appendix B of this report. A more detailed description of the six-degree-of-freedom program is given in reference 1. Results from these studies indicated that, for all constant wind-velocity profiles regardless of their magnitude and direction, the total wind effect occurred during the first 400 feet of flight. A more detailed study showed that small wind effects did exist above the altitude of 400 feet when a profile with wind velocity continually increasing with altitude was used.

Since meteorological data measured over the Eastern United States indicated an increase in wind velocity with altitude as a general trend, with peak velocities usually occurring at altitudes between 30,000 and 50,000 feet (ref. 2), wind-velocity gradients from 0 to 4 ft/sec per 1,000 feet of altitude were used in the IBM 704 electronic data processing machine from sea level to altitudes of approximately 40,000 feet. These studies showed that, in general, for a Little Joe type of vehicle, wind effects above 400 feet amounted to only a small percent of the total effect and approached zero as the wind gradient approached zero. Thus, a characteristic of this Little Joe vehicle is that 400 feet is considered the upper altitude limit for significant wind effect. Other vehicles

could have a different altitude of significant wind effect, depending upon the aerodynamic performance and inertia characteristics of the vehicle.

From the results of these Little Joe studies, it was decided to neglect the small wind effects above 400 feet and consider only winds below this altitude as having an effect on the flight of the vehicle. By considering only the wind effects below 400 feet, a rapid method for determining launcher corrections using wind data measured just prior to take-off could be developed.

In relation to the Little Joe program, it was estimated that the average wind-velocity gradient between sea level and an altitude of 40,000 feet, in which the average wind direction was such that the percent of the total wind effect that occurred above 400 feet could cause more than a 5° error in an azimuth correction and a 1° error in an elevation correction, would be considered the limiting wind-velocity gradient under which a flight test would be attempted. (Percentage wind effects are based on total wind effects which are assumed to occur between the ground and an altitude of 40,000 feet.) Wind gradients larger than this could at that time produce errors of such a magnitude as to be unacceptable to range safety and recovery operations.

Figures 9 and 10 show carpet plots of the percentage wind effects above the altitude of 400 feet as calculated for a Little Joe type of vehicle. These percentage effects vary with the size of the wind gradient and the direction of the gradient with respect to the vehicle. If the magnitude of the weighted wind-velocity gradient and its weighted direction prior to the time of a scheduled launching are known, the magnitude of the errors that could exist in the azimuth and elevation corrections due to wind effects above 400 feet can be determined from carpets similar to those in figures 9 and 10. For instance, if the products of correction angles in azimuth and elevation and the respective percentage effects are greater than the maximum allowable errors, the flight should be postponed until changing wind conditions cause the required corrections to fall within the accepted limits. From the experience gained from the four Little Joe flights, on an average flight day, errors in launcher setting due to wind effects above 400 feet are not expected to exceed 2° in azimuth or 0.5° in elevation.

As stated previously, the wind-effects investigation now under discussion was conducted on a vehicle having a take-off acceleration of 6g. Investigations using constant wind profiles for Little Joe vehicles with take-off accelerations higher than 6g showed that the altitude for total wind effect decreased with an increase in take-off acceleration. For a take-off acceleration of 10g, all changes in heading and flight-path angles for the Little Joe vehicle were shown to occur during the first 250 feet of flight.

METHOD OF CORRECTING A LAUNCHER SETTING FOR WIND EFFECTS

General

The results of the general study of wind effects on a Little Joe vehicle led to the development of a method of correcting a nominal launcher setting for wind effects. The procedure followed in the method of correcting for wind effects is briefly summarized in the following four steps:

(1) A specific wind-effects study using constant wind-velocity profiles at various directions relative to the vehicle is conducted with the six-degree-of-freedom program for the vehicle being flight tested. These profiles are programed from the ground up to a 40,000-foot altitude.

(2) Only winds up to the first few hundred feet of altitude are considered as having an effect on the trajectory of the vehicle. This altitude limit is the altitude where the vehicle has experienced all alterations in azimuth and elevation angle that are going to occur due to constant wind profiles and where vehicle damping begins. This limit is determined from the specific wind effects study. In the case of a take-off at 6g of a Little Joe vehicle, 400 feet is considered the upper altitude limit for wind effect. For a take-off at 10g, the upper limit is considered to be 250 feet.

(3) Carpet plots are constructed from the data of the specific wind-effects study. From these plots, correction angles in both the azimuth and elevation planes can be read directly for any given constant wind velocity and direction.

(4) Close to the time of launch, an average weighted wind velocity and direction is determined from wind measurements to represent the wind profile from the ground to the estimated maximum altitude of wind effect. This average weighted wind velocity and direction is then applied to the carpet plots, which yield the correction angles to be applied to the nominal launcher setting.

Study of Constant Wind-Velocity Effects

A specific study of the effects of constant wind-velocity profiles on the trajectory of a vehicle is required for all vehicles that differ in aerodynamic, acceleration, and inertia characteristics. This specific study provides the necessary data used in constructing carpet plots, which are used to determine correction angles for a nominal launcher setting to offset wind effects.

For three different elevation angles, three constant wind-velocity profiles are orientated in six different directions relative to the vehicle. This represents a total of 54 cases on the IBM machine. Three velocities and three launch angles are used since three points will determine the shape of their curves as well as set the limits that can be tolerated for these two variables. Since wind direction relative to the vehicle can vary 180°, from a tail wind to a head wind, six directions are used to insure the accuracy of the curve representing directional effects of winds on the vehicle.

G
4

Correction in the Azimuth Plane

The total changes in heading angle $\Delta\psi_T$ produced by a constant wind velocity from the six angles relative to the vehicle are first calculated. For a certain elevation angle at launch, the changes in heading angle are used to construct a plot similar to the one shown in figure 11 from which correction angles can be read. For this plot three wind velocities orientated in the six directions relative to the vehicle were used. The abscissa in figure 11 is the direction angle of the wind relative to the vehicle at launch. The ordinate is the direction angle of the wind relative to the vehicle after the addition of the change in heading angle produced by a given wind velocity has been made. This change in heading angle occurs in this case over the first 400 feet of flight. If the ordinate is considered the direction of the wind relative to the desired or nominal azimuth on which the vehicle is pointing, its corresponding value on the abscissa for a given wind velocity indicates where the launcher must be moved so that the wind effect will bring the vehicle back to its nominal azimuth heading at an altitude of approximately 400 feet. This is to say, to determine azimuth correction angles for different wind directions, start on the ordinate of figure 11 and find, for any wind velocity, its corresponding value on the abscissa. The difference in the two values is the correction angle which is applied to the nominal azimuth heading. This correction angle is always applied in a counterclockwise direction for a wind coming from the right of the launcher, and clockwise for a wind blowing from the left of the launcher. (See fig. 8.) Since three launch elevation angles are used for the specific wind-effects study, three plots (one for each elevation setting) similar to the one in figure 11 are necessary. From each of the three plots, correction angles in azimuth are recorded for the three wind velocities at various directions relative to the vehicle. Plotting these data in three-dimensional carpet form makes it possible to read a correction angle for any wind velocity and direction at any launch angle within the limits of the specific wind-effects study. Figure 12 is an example of a typical three-dimensional azimuth-correction carpet plot. For example, an elevation setting $\gamma = (m + 3)^\circ$, a wind velocity $V = 25n$ ft/sec, and a wind direction relative to the vehicle of 10°, give an azimuth correction

[redacted]

angle of 3.5°, which is located by arrows on figure 12. Information about the construction and reading of carpet plots can be found in reference 3.

Correction in the Elevation Plane

From the results of the general wind-effects study discussed in the section entitled "General Study of Wind Effects on a Little Joe Vehicle," it was found that the total response of the vehicle to a constant wind velocity took place within the first 400 feet of the vehicle's flight. The time from take-off corresponding to this altitude is approximately 3 seconds. It was found that the nominal no-wind trajectory could be duplicated with trajectories subjected to constant wind profiles, by repositioning the launcher. If, after 3 seconds of flight, the flight-path angle for the wind trajectory matched the flight-path angle for the nominal no-wind trajectory, the altitude and range parameters would be the same for both flights. Since the vehicle starts a period of damping as it reaches an altitude of 400 feet at approximately 3 seconds from take-off, 10 seconds from take-off was chosen as the time for comparison of flight-path angles between wind and no-wind trajectories to allow a conservative time interval of 7 seconds for damping.

From the specific wind-effects study, flight-path angles at 10 seconds after take-off were computed. Since the flight-path angle for the desired nominal no-wind trajectory is known at 10 seconds, a three-dimensional carpet plot using the computed flight-path angles at 10 seconds is constructed from which elevation corrections are determined for any constant wind velocity and direction relative to the vehicle.

Figure 13 is an example of a three-dimensional carpet plot constructed for launch angle correction in the elevation plane. A weighted constant wind velocity, its direction with respect to the vehicle, and the flight-path angle at 10 seconds for the nominal no-wind trajectory will give a point on the carpet from which the corrected elevation setting is determined. For an example, a wind velocity of 14n ft/sec, a flight-path angle at 10 seconds of 67°, and a wind-direction angle with respect to the vehicle of 50° give a corrected elevation angle of $(m + 3)^{\circ}$ at launch which is located by the arrow on figure 13.

Wind-Weighting Method

In order to represent a measured wind profile with a constant wind velocity and direction from the ground up to the required altitude, in this case 400 feet, a method of weighting the effects of wind with altitude was developed. Analysis of data obtained from the general wind-effects study showed that, over given increments of altitude from

the ground to the determined upper limit of altitude, the percentage change in heading and flight-path angles was approximately the same for all wind velocities, but varied with direction relative to the vehicle. Figure 14 is a carpet plot showing weighting factor as a function of altitude and wind direction relative to the vehicle. The weighting factors on this carpet are determined by combining the weighted percentage changes in flight-path angle and azimuth angle with respect to altitude for different wind directions. These percentage changes in both azimuth and elevation are weighted by applying directional sensitivity factors since the intensity of the wind effect is not the same in both planes for a given wind direction. Tables V to VIII show numerically how the weighting factors in figure 14 were determined. Table V shows the change in heading and flight-path angles for different altitude increments up to 400 feet and at five wind directions relative to the rocket vehicle. The total change in heading and flight-path angles ($\Delta\psi_T$ and $\Delta\gamma_T$) for each wind direction are shown on the last row of table V. Table VI shows the percentage change in heading and flight-path angles $\left(\frac{\Delta\psi}{\Delta\psi_T} \text{ and } \frac{\Delta\gamma}{\Delta\gamma_T}\right)$ for the different altitude increments at the five wind directions. Table VII shows how sensitivity factors for five wind directions in the azimuth and elevation planes are determined from $\Delta\psi_T$ and $\Delta\gamma_T$. Using the sensitivity factors for the five wind directions in both azimuth and elevation, applying these factors to the percentage change in heading and flight-path angles from table VI, and summing the results for each wind direction give weighting factors at different levels of altitude for the five wind directions. These data are presented in table VIII and are shown graphically in figure 14. Since figure 14 is a carpet plot, it is possible to determine a weighting factor for any altitude increment up to 400 feet at any wind direction. A carpet plot similar to the one in figure 14 is constructed from the data of a specific wind-effects study (see section entitled "Study of Constant Wind-Velocity Effects") for each vehicle that differs in aerodynamic performance and take-off acceleration.

For any wind speed and direction relative to the vehicle, a weighting factor can be determined for any desired interval of altitude between the ground and upper limit, in this case 400 feet. Average velocities and directions can be determined for linear steps along the measured wind-velocity and direction profiles. Weighting factors are determined for the average wind direction of each step and applied to the average velocity of that step. The number of altitude increments needed for obtaining a constant weighted wind velocity and direction over the altitude range being considered depends entirely on the linearity of the measured wind-velocity profile.

The average weighted wind velocities and directions for each altitude step are resolved into component form and summed. The final resultant

is a constant weighted wind velocity and direction which is considered representative of the profile that exists near the time of launch. An example of the weighting procedure is shown in figure 15. The table and indicated steps show how this particular profile would be weighted. The weighting factors shown in figure 15 were taken from a plot similar to the one shown in figure 14.

OPERATIONAL APPLICATION OF THE METHOD OF CORRECTING LAUNCHER SETTINGS FOR WIND EFFECTS

In order to minimize the time required to locate points on both three-dimensional correction-angle carpet plots as well as to minimize the chance of error in locating these points, two-dimensional carpets are constructed from the two three-dimensional carpets. The third dimension on the azimuth-correction carpet is elevation angle at launch γ; therefore, two-dimensional carpets for every degree of elevation angle at launch can be constructed between the upper and lower elevation limits. This procedure has resulted in 10 carpet plots in the past. Wind velocity is the third dimension on the elevation-correction carpet, so it follows that two-dimensional carpets for increments of 1 ft/sec of wind velocity from zero to the upper limit can be constructed. Linear interpolation can be used between each degree of elevation angle and every increment of wind velocity of the two-dimensional carpets. The operational need for this number of curves in helping to simplify and speed up the readout capabilities of the correction method explains the importance of carpet plotting. From a minimum number of points obtained from the IBM machine, two three-dimensional carpet plots can be constructed from which an infinite number of interpolated and extrapolated values can be obtained.

Prior to the time of launch, all necessary two-dimensional correction carpets, high-altitude wind-effect carpets, and a wind-weighting carpet are prepared. Experience has shown that approximately 3 hours before launch, a chaff balloon should be released and tracked by radar to an altitude of approximately 50,000 feet. By using the radar plotboard, wind velocities and directions are determined up to this altitude. A wind gradient and wind direction determined from the measured data of this high-altitude balloon are used in calculating the percentage wind effects in azimuth and elevation that could be expected above a predetermined altitude, 400 feet in the case of the booster having a take-off acceleration of 6g. These high-altitude percentage wind effects are found by using the upper-altitude percentage wind-effect carpet plot already prepared. The time involved in tracking this high-altitude balloon and reducing the data is approximately $1\frac{1}{2}$ to 2 hours.

While the plotboard data for the high-altitude balloon are being reduced, weighted wind velocities and directions can be determined every $\frac{1}{2}$ hour over the important first few hundred feet of altitude. These values are found from data read directly from wind-reading instruments located on a meteorological tower. If a meteorological tower is not available, these data for wind profiles can be determined from chaff balloons tracked by radar over the first few hundred feet of altitude. It is recommended that approximately 1 hour before take-off, an initial corrected launcher setting from that of the nominal setting should be determined. This step is taken to determine whether the required settings are within the mechanical limitations of the launcher. If not, a "hold" must be initiated until wind conditions are acceptable. The latest average weighted wind velocity and direction can be located at a point on the azimuth-correction carpet plot for the desired or nominal elevation angle at launch, and a correction angle found. Applying this correction in azimuth will change the direction of the wind with respect to the vehicle. From this new wind direction relative to the vehicle, the average weighted wind velocity, and the flight-path angle at 10 seconds for the nominal no-wind trajectory, an elevation correction can be determined. By using the desired azimuth once again and the new elevation setting, a new azimuth correction is determined. With the new azimuth correction, another elevation correction is determined. This iteration process is repeated until a correction in azimuth causes no change in elevation setting. Since a large change in azimuth causes a relatively small change in elevation, this iteration process is quite rapid with the values converging within the first two or three steps. By using the initial corrected launcher setting, the percentage wind effects above the predetermined altitude level, say 400 feet in this case, should be determined. If the high-altitude effects cause no larger than a 5° error in azimuth correction and a 1° error in elevation correction, and the average weighted wind velocity falls within its predetermined limits, a final launcher setting should be determined with the procedure just described, using wind data measured less than $\frac{1}{2}$ hour before take-off. From the time of final launcher setting to the time of take-off, meteorological instruments at a variety of altitude levels should be monitored to note any change in the low-altitude wind profile from that used for final launcher corrections. If a large shift in wind velocity or direction is noted, the countdown should be held until new correction angles can be determined.

Since wind data are only required for the first few hundred feet of altitude, a meteorological tower with wind-measuring equipment at different levels would provide the optimum in efficiency. By reading wind velocities and directions directly from the tower, the time required to calculate correction angles would be of the order of 10 minutes. If

a chaff balloon is used to measure the low-altitude winds, the time required to calculate correction angles is doubled due to the time spent in tracking the balloon and reducing the data from the radar plotboard. Due to the absence of a meteorological tower, the chaff-balloon method was used to determine low-altitude wind profiles for the four Little Joe flight tests utilizing this correction method. Results and discussion of these four flight tests are found in appendix A.

CONCLUDING REMARKS

A method of estimating launcher settings to compensate for effects of winds on the trajectory of a Little Joe rocket vehicle has been developed and used on four Little Joe flight tests. This method can be applied to other fin-stabilized rocket vehicles having aerodynamic, performance, and inertia characteristics similar to those of the Little Joe booster.

The method of correcting a nominal launcher setting to compensate for wind effects was developed from theoretical studies using six-degree-of-freedom equations of motion programed into a trajectory simulation program. The results of the four flight tests indicate that the method is quite satisfactory for controlling the booster phase of flight.

Space Task Group,
National Aeronautics and Space Administration,
Langley Field, Va., October 13, 1960.

DECLASSIFIED

APPENDIX A

FLIGHT-TEST RESULTS

Four Little Joe vehicles have been flown by use of the launcher-correction method presented in this report. Three of the four flight tests differed in take-off acceleration, making three sets of correction data necessary. The nominal or desired conditions, the corrected conditions, and the achieved conditions are presented in table IX. Weighted wind velocities and directions and the altitude of total wind effects are also shown in this table.

The results from the flight tests indicate that the launcher-correction method is quite adequate in guiding the booster phase of flight. The high-altitude wind profiles for the four Little Joe flight tests are shown in figures 16 to 19. Figure 17 shows the measured wind profile from the ground to an altitude of 26,000 feet on the day of the second Little Joe flight test. As indicated in table IX, the altitude of total wind effect was considered to be the first 250 feet. The average weighted wind velocity and direction was found to be 29 ft/sec and 206° from true north, respectively, over this altitude. However, as seen in figure 17, the wind velocity increases to a relatively constant value of approximately 50 ft/sec at 1,000 feet and continues at this value to approximately 20,000 feet. As seen in table IX, the measured flight results show quite a close comparison with nominal or desired conditions, an indication that the launcher corrections were adequate and accurate. Since the increase in wind velocity at altitudes above 250 feet appeared to have no noticeable effect on the flight of the Little Joe vehicle during the second flight test, the theoretical assumption that all noticeable wind effect occurs over the first few hundred feet of the vehicle's flight trajectory is considered reasonable. Further verification of this assumption was found on the fourth Little Joe flight test. As in the case of second flight test of a Little Joe vehicle figure 19 shows a large increase in wind velocity at altitudes above 250 feet. These increased wind velocities appeared to have no noticeable effect on the flight trajectory of the Little Joe vehicle in the fourth flight test.

As stated earlier in the body of this report, errors in launcher setting due to wind effects at altitudes above 400 feet on an average flight day are not expected to exceed 2° in azimuth and 0.5° in elevation. The average wind gradients measured before each of the four Little Joe flight tests are shown in table IX. The maximum calculated error in azimuth due to wind effects at altitudes above 400 feet occurred on the second Little Joe flight test where the applied azimuth correction angle was 24°. The calculated error in the azimuth correction due to the wind

effects above 400 feet was approximately 2.5°. Calculated errors in azimuth correction on the other three flight tests were less than 0.5°. The maximum calculated error in launcher correction in elevation due to wind effects above 400 feet occurred on the fourth Little Joe flight test where a 7° correction angle was applied to the initial elevation setting. The calculated error in correction angle due to the wind effects above 400 feet was approximately 0.6°. Calculated errors in elevation correction on the other three flight tests were less than 0.3°. These numbers and the results of the four flight tests tend to support the assumption behind this correction method that the rocket vehicle will fly extremely close to the desired or nominal trajectory if the low-altitude winds only are considered as affecting the flight of the vehicle and these effects are adequately compensated for.

DECLASSIFIED

APPENDIX B

EQUATIONS OF MOTION

The six-degree-of-freedom analysis discussed in reference 1 has been modified for use on the Little Joe program by the NASA Space Task Group. Symbols used in the equations of motion which have not been defined previously are included in the following list:

A	cross-sectional area
a, b, c	thrust-force direction cosines
C_A	aerodynamic force coefficient along body X-axis as a function of η and M
$C_{A,O}$	aerodynamic force coefficient along body X-axis when $\eta = 0^o$
$C_{m_{\dot{\eta}}}$	rate of change of pitching-moment coefficient with time rate of change of combined wind angle, $\frac{dC_m}{d\left(\frac{\dot{\eta}D}{2V'}\right)}$
C_N	aerodynamic force coefficient normal to body X-axis as a function of η and M
D	any diameter, ft
I_X, I_Y, I_Z	mass moments of inertia about body axes, slug-ft^2
I_{XZ}	product of inertia, slug-ft^2
m	mass, slugs
p, q, r	components of ω about X-, Y-, Z-axes, respectively
q'	free-stream dynamic pressure, $\frac{1}{2}\rho(V')^2$, lb/sq ft
u, v, w	components of inertial velocity along body X-, Y-, Z-axes, respectively, ft/sec
u', v', w'	velocity components of V' along body X-, Y-, Z-axes, respectively, which include wind profile

V' velocity of vehicle relative to moving air mass, ft/sec

x_{cg} center-of-gravity distance from nose, ft

x_{cp} center-of-pressure distance from nose, ft

$\alpha = \tan^{-1}\left(\frac{w'}{u'}\right)$

$\beta = \tan^{-1}\left(\frac{v'}{u'}\right)$

η flow incidence angle, $\tan^{-1}\frac{\sqrt{(v')^2 + (w')^2}}{u'}$, radians

θ, ϕ Euler angles

$$\phi' = \sin^{-1}\frac{v'}{\sqrt{(v')^2 + (w')^2}} = \cos^{-1}\frac{w'}{\sqrt{(v')^2 + (w')^2}}$$

ρ free-stream atmospheric density, slugs/cu ft

ω inertial angular velocity, radians/sec

Dots over symbols denote derivatives with respect to time.

The six-degree-of-freedom analysis used for the Little Joe study was developed from the following equations of motion:

$$m(\dot{u} - vr + wq) = Fa - mg \sin\theta - \left(C_{A,0} + C_A\right)q'A$$

$$m(\dot{v} - wp + ur) = Fb + mg \sin\phi \cos\theta - C_N q'A \sin\phi'$$

$$m(\dot{w} - uq + vp) = Fc + mg \cos\phi \cos\theta - C_N q'A \cos\phi'$$

DECLASSIFIED

$$\dot{p}I_X - \dot{r}I_{XZ} + (I_Z - I_Y)qr - pqI_{XZ} = 0$$

$$\dot{q}I_Y + rp(I_X - I_Z) + (p^2 - r^2)I_{XZ} = \left[C_{m_{\dot{\eta}}} \frac{\dot{\eta}D}{2V'} q'AD + C_N(x_{cp} - x_{cg})\right] \cos \phi'$$

$$\dot{r}I_Z - \dot{p}I_{XZ} + (I_Y - I_X)pq + I_{XZ}qr = \left[C_{m_{\dot{\eta}}} \frac{\dot{\eta}D}{2V'} q'AD - C_N(x_{cp} - x_{cg})\right] \sin \phi'$$

G
4

[redacted]

REFERENCES

1. James, Robert L., Jr. (With appendix B by Norman L. Crabill): A Three-Dimensional Trajectory Simulation Using Six Degrees of Freedom With Arbitrary Wind. NASA TN D-641, 1961.

2. Sissenwine, Norman: Development of Missile Design Wind Profiles for Patrick AFB. Air Force Surveys in Geophysics No. 96 (AFCRC-TN-58-216, ASTIA Doc. No. AD.146870), Air Force Cambridge Res. Center, Mar. 1958.

3. Yates, A. H.: 'Carpets' and 'Lattices'. Aircraft Engineering, vol. XVIII, no. 203, Jan. 1946, pp. 8-9.

TABLE I.- WIND-TUNNEL DATA OF POWER-ON DRAG COEFFICIENT

M	C_D at –					
	$\alpha = 0^\circ$	$\alpha = 10^\circ$	$\alpha = 30^\circ$	$\alpha = 60^\circ$	$\alpha = 90^\circ$	$\alpha = 110^\circ$
0.40	0.90	1.21	3.13	5.17	7.39	6.74
.80	1.10	1.45	3.35	5.40	7.61	6.96
1.00	1.38	1.78	3.73	5.83	8.11	7.46
2.10	.68	1.03	3.06	5.30	7.71	7.06
4.65	.39	.72	2.73	4.92	7.28	6.63
6.83	.21	.51	2.50	4.68	7.03	6.38

CONFIDENTIAL

CONFIDENTIAL

TABLE II.- WIND-TUNNEL DATA OF POWER-OFF DRAG COEFFICIENT

M	C_D at —					
	$\alpha = 0^\circ$	$\alpha = 10^\circ$	$\alpha = 30^\circ$	$\alpha = 60^\circ$	$\alpha = 90^\circ$	$\alpha = 110^\circ$
0.40	0.57	0.92	2.90	5.06	7.39	6.74
.80	.75	1.14	3.12	5.28	7.61	6.96
1.00	1.22	1.64	3.62	5.78	8.11	7.46
2.10	.92	1.24	3.22	5.38	7.71	7.06
4.65	.49	.81	2.79	4.95	7.28	6.63
6.83	.27	.56	2.54	4.70	7.03	6.38

TABLE III.- WIND-TUNNEL DATA OF LIFT COEFFICIENT

M	C_L at −					
	$\alpha = 0^\circ$	$\alpha = 10^\circ$	$\alpha = 30^\circ$	$\alpha = 60^\circ$	$\alpha = 90^\circ$	$\alpha = 110^\circ$
0.40	0	1.99	4.63	2.39	-0.32	-2.70
.80	0	2.10	4.74	2.50	-.21	-2.59
1.00	0	2.30	4.94	2.70	-.01	-2.39
2.10	0	1.54	4.18	1.94	-.77	-3.15
4.65	0	1.04	3.68	1.44	-1.27	-3.65
6.83	0	0.91	3.68	1.44	-1.27	-3.65

CONFIDENTIAL

TABLE IV.- WIND-TUNNEL DATA OF PITCHING-MOMENT COEFFICIENT

[Moments were measured about station 372.9 shown on figure 1]

M	C_m at –					
	$\alpha = 0^\circ$	$\alpha = 10^\circ$	$\alpha = 30^\circ$	$\alpha = 60^\circ$	$\alpha = 90^\circ$	$\alpha = 110^\circ$
0.40	0	-2.45	-4.36	-0.46	-4.83	-8.01
.80	0	-2.72	-4.63	-.73	-5.10	-8.28
1.00	0	-3.36	-5.27	-1.37	-5.75	-8.92
2.10	0	-1.61	-3.52	.38	-3.99	-7.17
4.65	0	-.46	-2.37	1.35	-2.84	-6.02
6.83	0	-.31	-2.22	1.69	-2.69	-5.87

CONFIDENTIAL

TABLE V.- CHANGE IN HEADING AND FLIGHT-PATH ANGLES FOR DIFFERENT ALTITUDE INCREMENTS AT VARIOUS WIND DIRECTIONS WITH RESPECT TO THE ROCKET VEHICLE

h, ft	$\psi = 0^\circ$		$\psi = 45^\circ$		$\psi = 90^\circ$		$\psi = 135^\circ$		$\psi = 180^\circ$	
	$\Delta\psi$, deg	$\Delta\gamma$, deg	$\Delta\psi$, deg	$\Delta\gamma$, deg	$\Delta\psi$, deg	$\Delta\gamma$, deg	$\Delta\psi$, deg	$\Delta\gamma$, deg	$\Delta\psi$, deg	$\Delta\gamma$, deg
0 to 50	0	0.494	2.370	0.380	2.640	0	1.82	0.360	0	0.570
0 to 100	0	.755	2.850	.620	4.840	.110	3.20	.450	0	.815
0 to 150	0	1.500	7.000	1.020	7.150	.256	5.72	1.040	0	1.720
0 to 200	0	2.550	12.000	1.550	12.200	.392	8.00	1.840	0	2.930
0 to 250	0	3.880	17.600	2.410	18.000	1.040	11.60	2.820	0	4.530
0 to 300	0	4.650	21.300	2.750	22.000	1.170	13.10	3.370	0	5.300
0 to 350	0	5.050	24.400	2.960	23.500	1.330	14.20	3.740	0	5.850
0 to 400	0	5.800	28.000	3.300	26.400	1.700	15.0	4.500	0	6.800

CONFIDENTIAL

CONFIDENTIAL

TABLE VI.- PERCENTAGE CHANGE IN HEADING AND FLIGHT-PATH ANGLES FOR DIFFERENT ALTITUDE INCREMENTS AT VARIOUS WIND DIRECTIONS WITH RESPECT TO THE ROCKET VEHICLE

h, ft	$\psi = 0^\circ$	$\psi = 45^\circ$		$\psi = 90^\circ$		$\psi = 135^\circ$		$\psi = 180^\circ$
	$\frac{\Delta\gamma}{\Delta\gamma_T}$	$\frac{\Delta\psi}{\Delta\psi_T}$	$\frac{\Delta\gamma}{\Delta\gamma_T}$	$\frac{\Delta\psi}{\Delta\psi_T}$	$\frac{\Delta\gamma}{\Delta\gamma_T}$	$\frac{\Delta\psi}{\Delta\psi_T}$	$\frac{\Delta\gamma}{\Delta\gamma_T}$	$\frac{\Delta\gamma}{\Delta\gamma_T}$
0 to 50	0.085	0.085	0.115	0.100	0	0.121	0.080	0.084
0 to 100	.130	.102	.187	.183	.065	.213	.100	.120
0 to 150	.260	.250	.310	.271	.150	.382	.230	.253
0 to 200	.440	.430	.470	.462	.230	.531	.410	.430
0 to 250	.670	.631	.731	.681	.610	.774	.627	.665
0 to 300	.800	.760	.834	.832	.690	.874	.750	.780
0 to 350	.870	.870	.891	.891	.780	.942	.830	.860
0 to 400	1.000	1.000	1.000	1.000	1.000	1.000	1.000	1.000

TABLE VII.- SENSITIVITY FACTORS FOR VARIOUS WIND DIRECTIONS IN THE AZIMUTH AND ELEVATION PLANES

$\left[\Sigma\ \Delta\psi_T = 69.40;\ \Sigma\ \Delta\gamma_T = 22.10\right]$

ψ, deg	$\Delta\psi_T$, deg	$\Delta\gamma_T$, deg	$\frac{\Delta\psi_T}{\Sigma\ \Delta\psi_T}$	$\frac{\Delta\gamma_T}{\Sigma\ \Delta\gamma_T}$	$\frac{\Delta\psi_T}{\Sigma\ \Delta\psi_T} + \frac{\Delta\gamma_T}{\Sigma\ \Delta\gamma_T}$	$\frac{\frac{\Delta\psi_T}{\Sigma\ \Delta\psi_T}}{\frac{\Delta\psi_T}{\Sigma\ \Delta\psi_T} + \frac{\Delta\gamma_T}{\Sigma\ \Delta\gamma_T}} = r$	$\frac{\frac{\Delta\gamma_T}{\Sigma\ \Delta\gamma_T}}{\frac{\Delta\psi_T}{\Sigma\ \Delta\psi_T} + \frac{\Delta\gamma_T}{\Sigma\ \Delta\gamma_T}} = s$
0	0	5.80	0	0.263	0.263	0	1.000
45	28.00	3.30	.405	.149	.554	.730	0.270
90	26.40	1.70	.380	.077	.457	.842	.158
135	15.00	4.50	.216	.204	.420	.515	.485
180	0	6.80	0	.307	.307	0	1.000

CONFIDENTIAL

CONFIDENTIAL

TABLE VIII.- WEIGHTING FACTORS FOR DIFFERENT ALTITUDE INCREMENTS AT VARIOUS WIND DIRECTIONS RELATIVE TO THE ROCKET VEHICLE

h, ft	$\psi = 0^\circ$			$\psi = 45^\circ$			$\psi = 90^\circ$			$\psi = 135^\circ$			$\psi = 180^\circ$		
	$\frac{\Delta\psi}{\Delta\psi_T}$ r	$\frac{\Delta\gamma}{\Delta\gamma_T}$ s	$\frac{\Delta\psi}{\Delta\psi_T}$ r + $\frac{\Delta\gamma}{\Delta\gamma_T}$ s	$\frac{\Delta\psi}{\Delta\psi_T}$ r	$\frac{\Delta\gamma}{\Delta\gamma_T}$ s	$\frac{\Delta\psi}{\Delta\psi_T}$ r + $\frac{\Delta\gamma}{\Delta\gamma_T}$ s	$\frac{\Delta\psi}{\Delta\psi_T}$ r	$\frac{\Delta\gamma}{\Delta\gamma_T}$ s	$\frac{\Delta\psi}{\Delta\psi_T}$ r + $\frac{\Delta\gamma}{\Delta\gamma_T}$ s	$\frac{\Delta\psi}{\Delta\psi_T}$ r	$\frac{\Delta\gamma}{\Delta\gamma_T}$ s	$\frac{\Delta\psi}{\Delta\psi_T}$ r + $\frac{\Delta\gamma}{\Delta\gamma_T}$ s	$\frac{\Delta\psi}{\Delta\psi_T}$ r	$\frac{\Delta\gamma}{\Delta\gamma_T}$ s	$\frac{\Delta\psi}{\Delta\psi_T}$ r + $\frac{\Delta\gamma}{\Delta\gamma_T}$ s
0 to 50	0	0.085	0.085	0.062	0.031	0.093	0.084	0	0.084	0.063	0.039	0.102	0	0.084	0.084
0 to 100	0	.130	.130	.074	.051	.125	.154	.013	.167	.110	.049	.159	0	.120	.120
0 to 150	0	.260	.260	.182	.084	.266	.228	.024	.252	.196	.112	.308	0	.253	.253
0 to 200	0	.440	.440	.315	.127	.442	.389	.036	.425	.273	.199	.472	0	.430	.430
0 to 250	0	.670	.670	.461	.197	.658	.574	.097	.671	.400	.304	.704	0	.665	.665
0 to 300	0	.800	.800	.555	.225	.780	.700	.109	.809	.450	.364	.814	0	.780	.780
0 to 350	0	.870	.870	.635	.240	.875	.750	.123	.873	.485	.403	.888	0	.860	.860
0 to 400	0	1.000	1.000	.730	.270	1.000	.842	.158	1.000	.515	.485	1.000	0	1.000	1.000

TABLE IX.- DESIRED, CORRECTED, AND ACHIEVED CONDITIONS FOR FOUR LITTLE JOE FLIGHT TESTS

Little Joe flight test	Desired conditions			Average weighted wind conditions			Launcher setting compensating for wind effects		Conditions achieved during flight			Measured average wind-velocity gradient
	Λz_n, deg	γ_n, deg	γ_{nt}, deg	θ_W, deg	$\bar{V}_W$, ft/sec	Altitude of wind effect, ft	Λz_c, deg	γ_c, deg	Λz_a, deg	γ_a, deg	γ_{at}, deg	G, $\frac{\text{ft/sec}}{1{,}000\ \text{ft}}$
First	110	80	67	220	16	400	94	78	106.0	80.3	67.6	0.184
Second	135	75	64	206	29	250	111	76	137.1	75.4	65.0	1.400
Third	140	82	72	5	20	300	157	78	138.5	80.1	68.2	.685
Fourth	135	77	68	315	36	250	135	70	133.0	76.7	67.4	.850

CONFIDENTIAL

CONFIDENTIAL

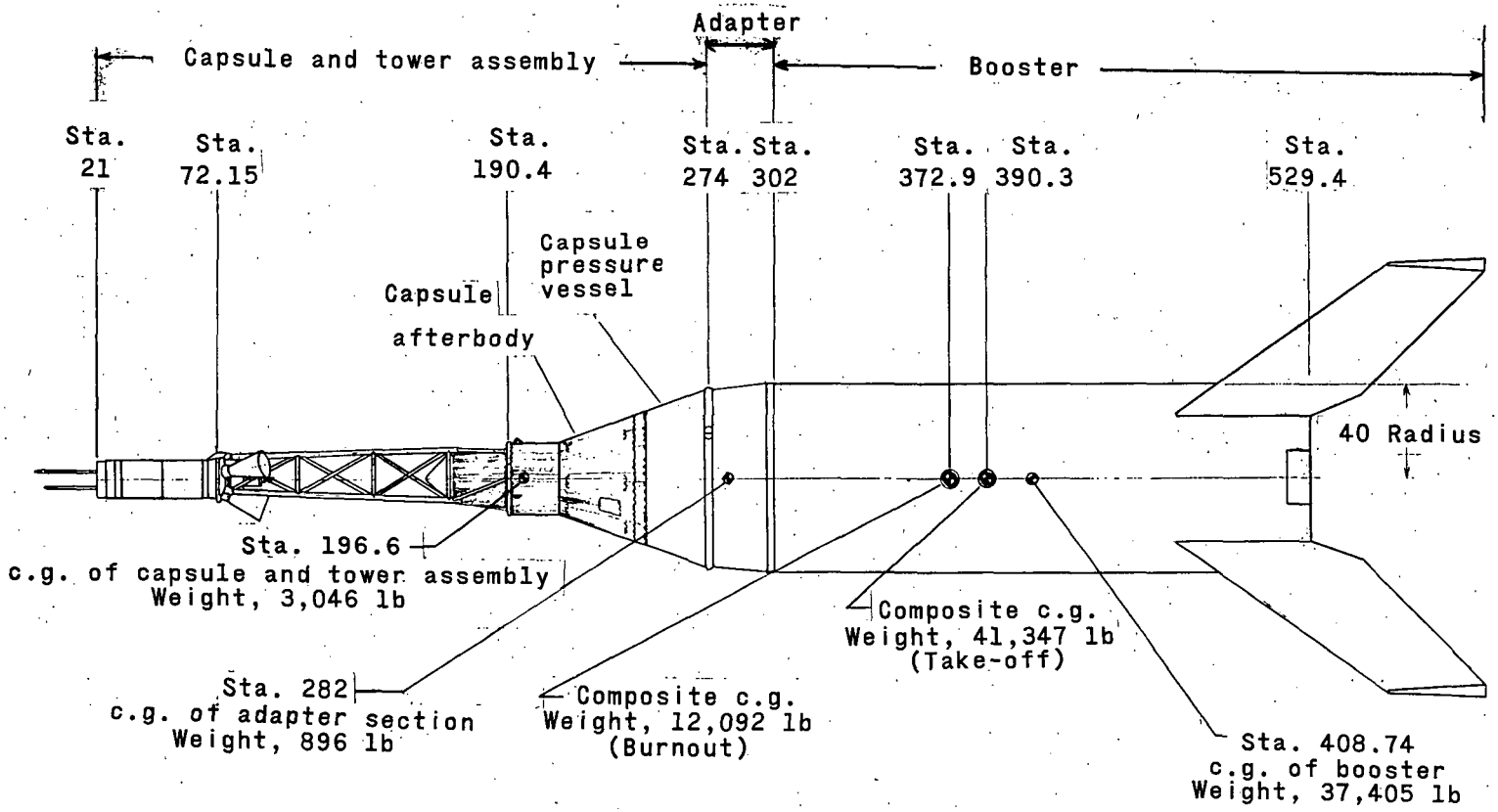

Figure 1.- External configuration of typical Little Joe vehicle. All dimensions are in inches.

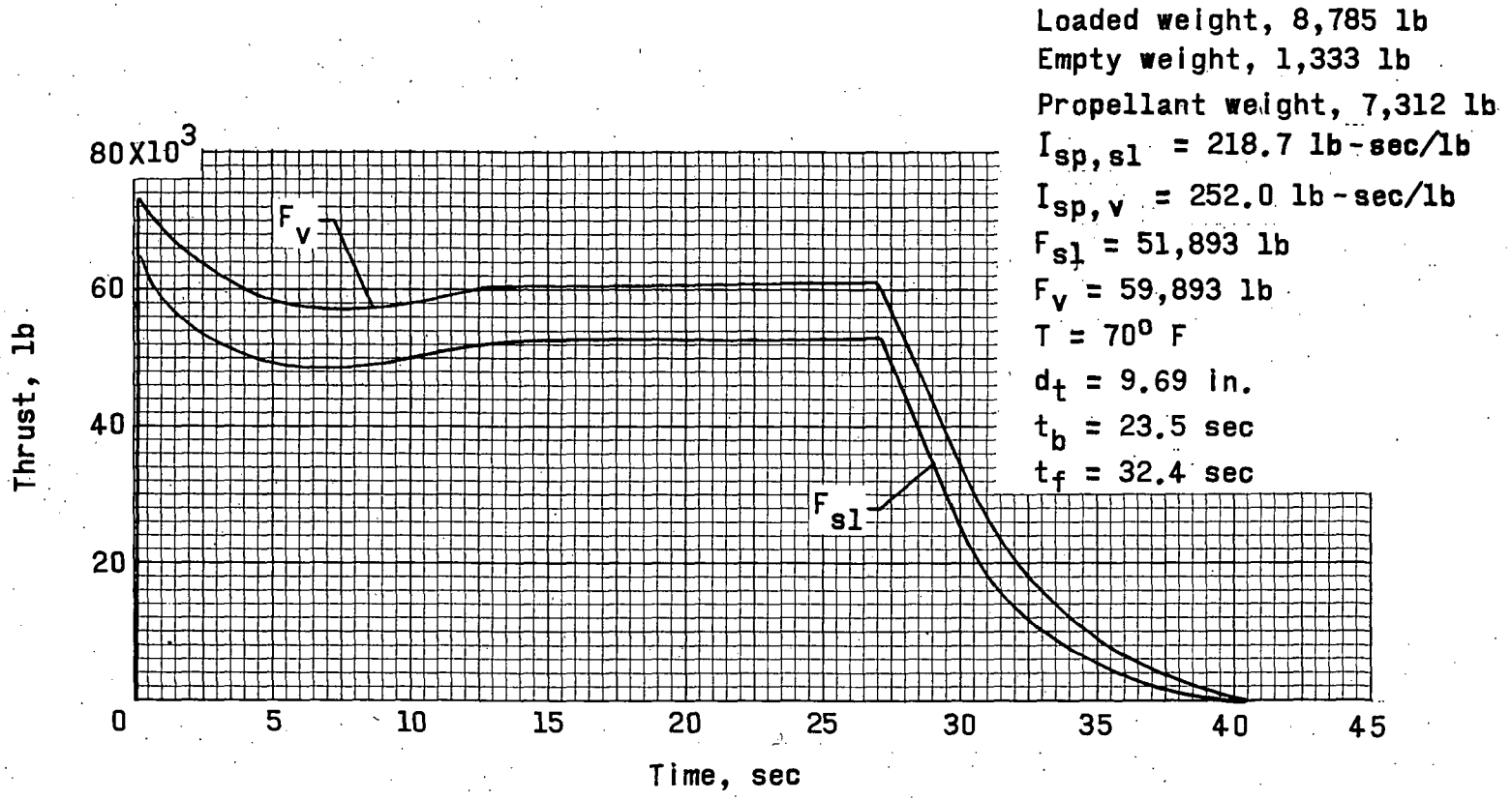

Figure 2.- Variation of axial thrust of typical Castor rocket motor with time. Nozzle canted 11° with reference to longitudinal axis of motor.

CONFIDENTIAL

CONFIDENTIAL

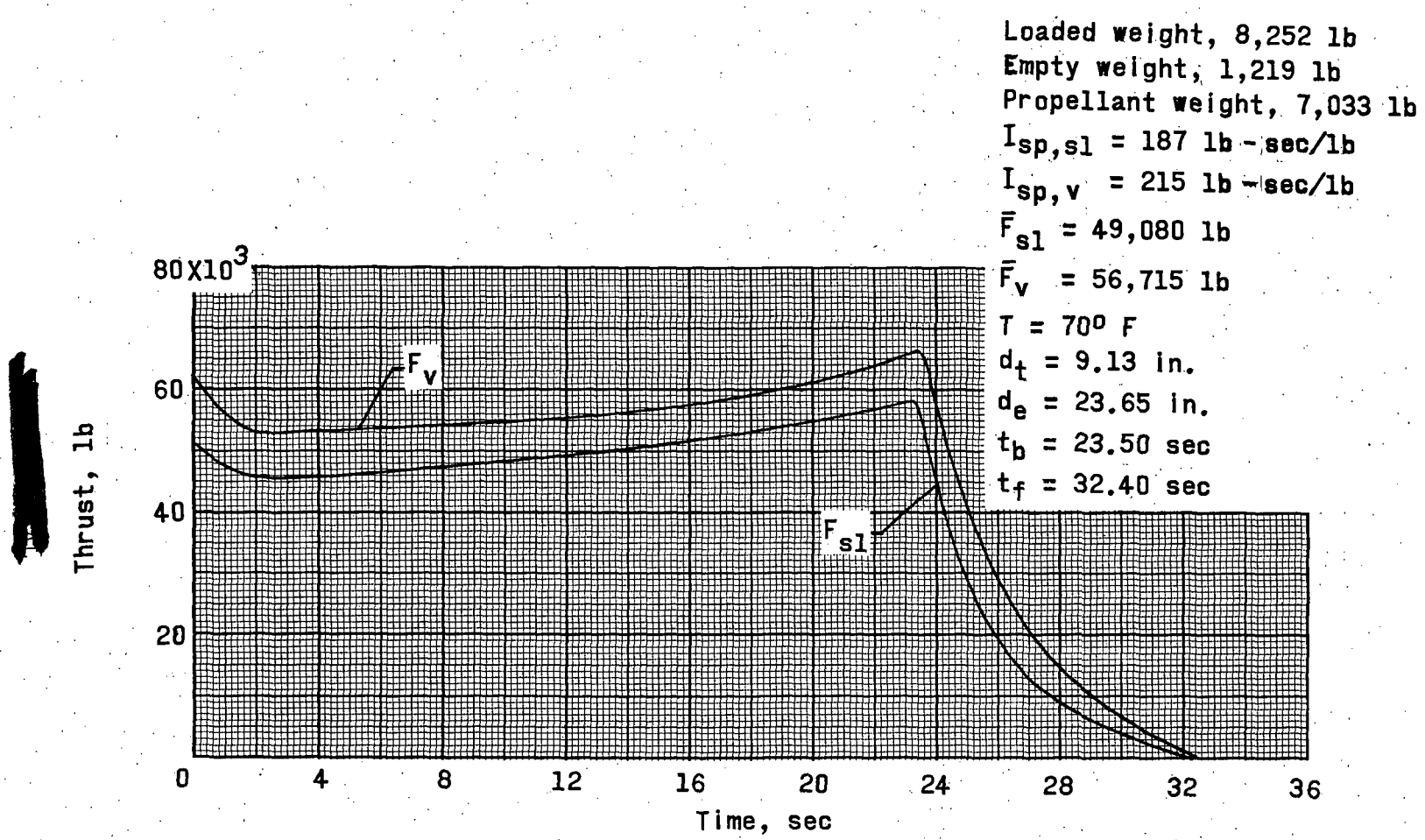

Figure 3.- Variation of axial thrust of typical Pollux rocket motor with time. Nozzle canted 11° with reference to longitudinal axis of motor.

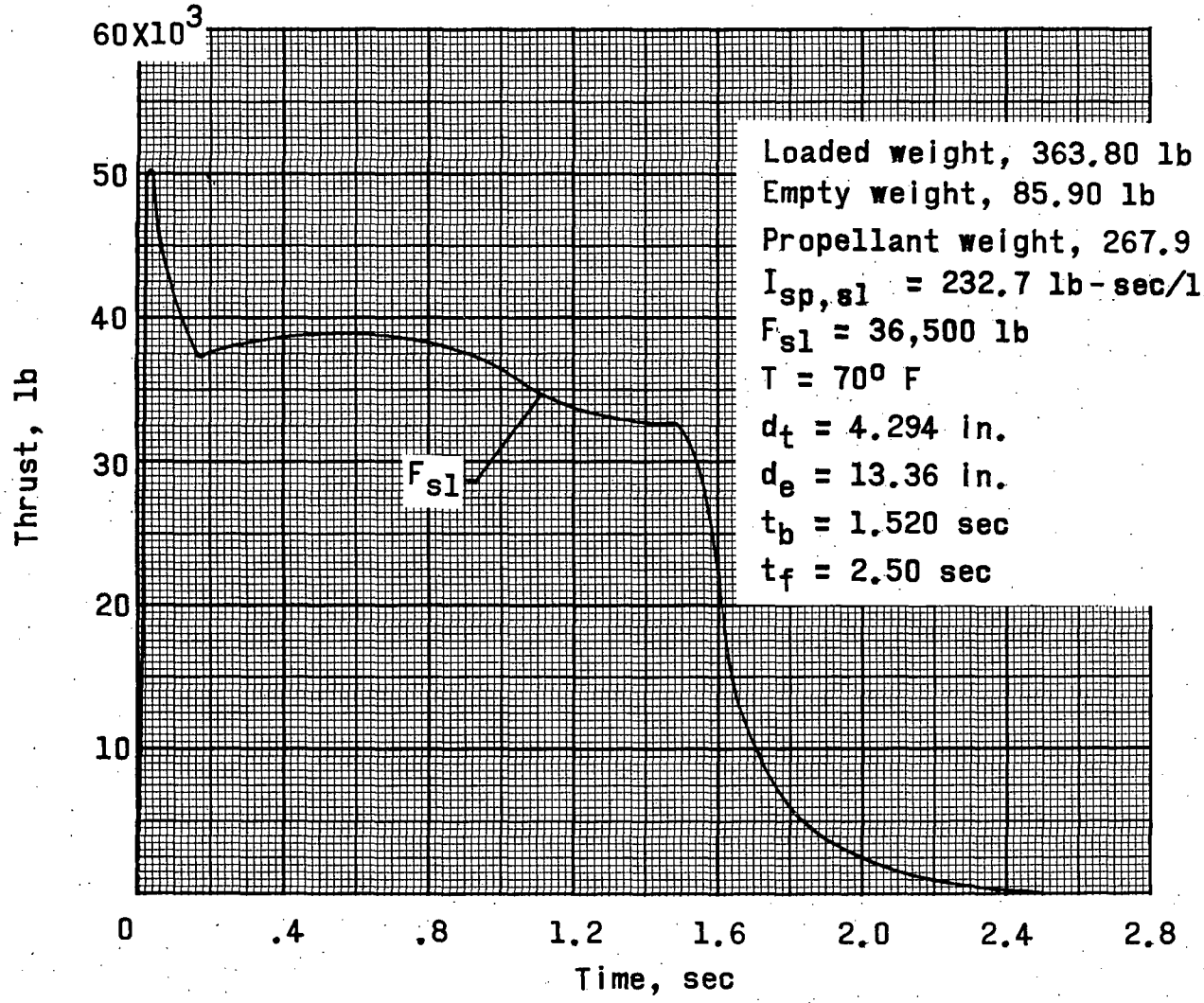

Figure 4.- Variation of axial thrust of typical Recruit rocket motor with time. Nozzle canted 12° with reference to longitudinal axis of motor.

CONFIDENTIAL

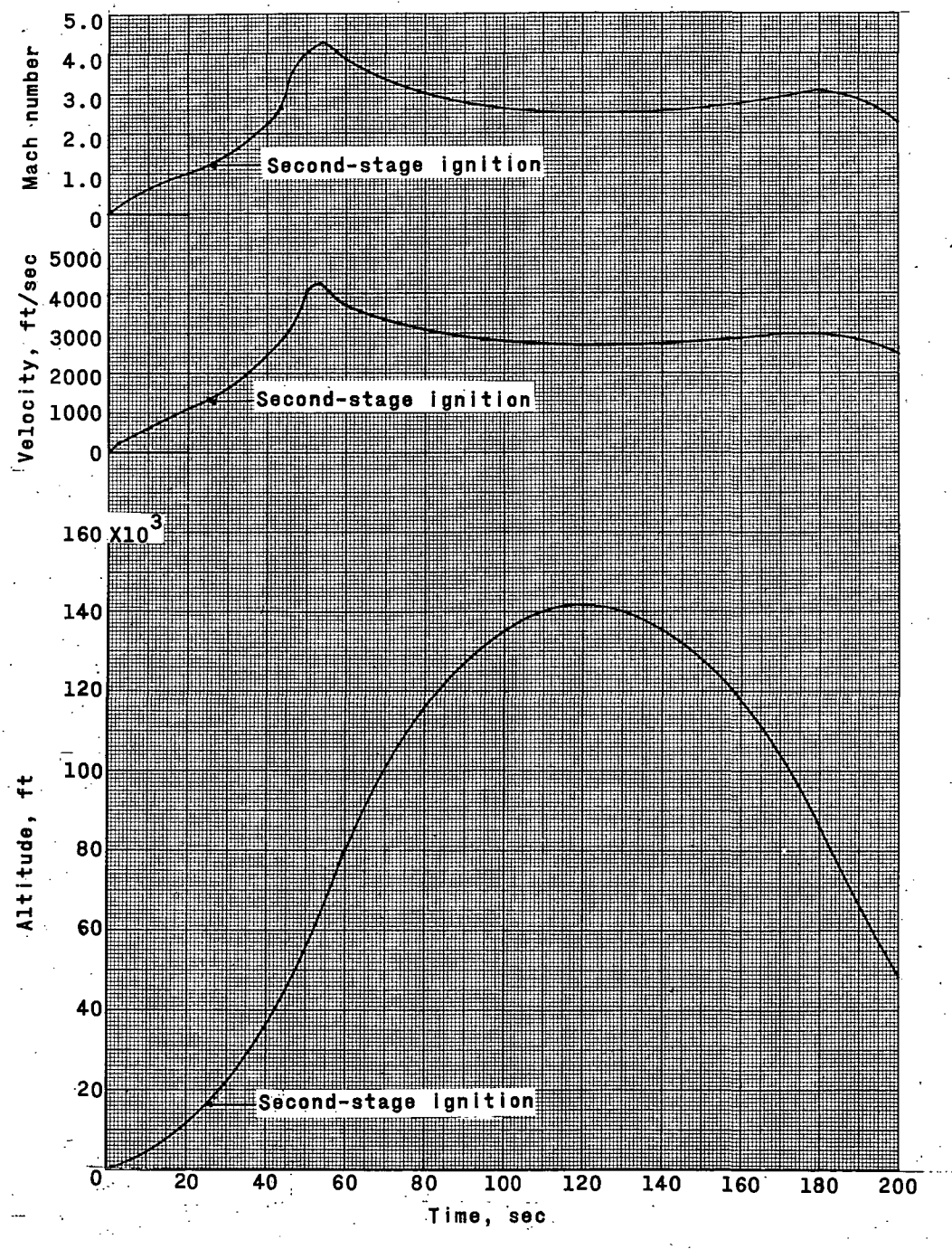

igure 5.- Time history of calculated altitude, velocity, and Mach number for Little Joe vehicle having a combination of four Recruit and four Pollux rocket motors.

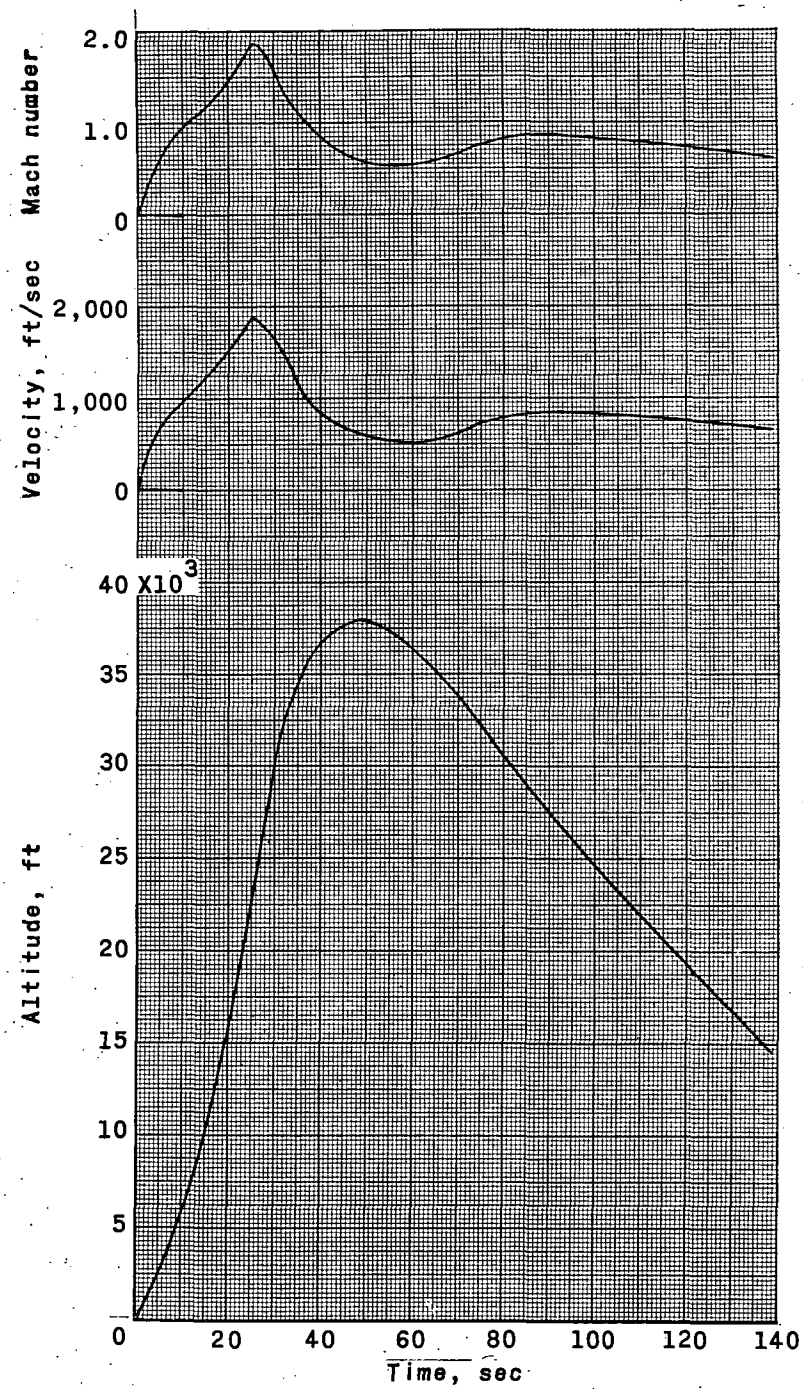

Figure 6.- Time history of calculated altitude, velocity, and Mach number for Little Joe vehicle having a combination of four Recruit and two Pollux rocket motors.

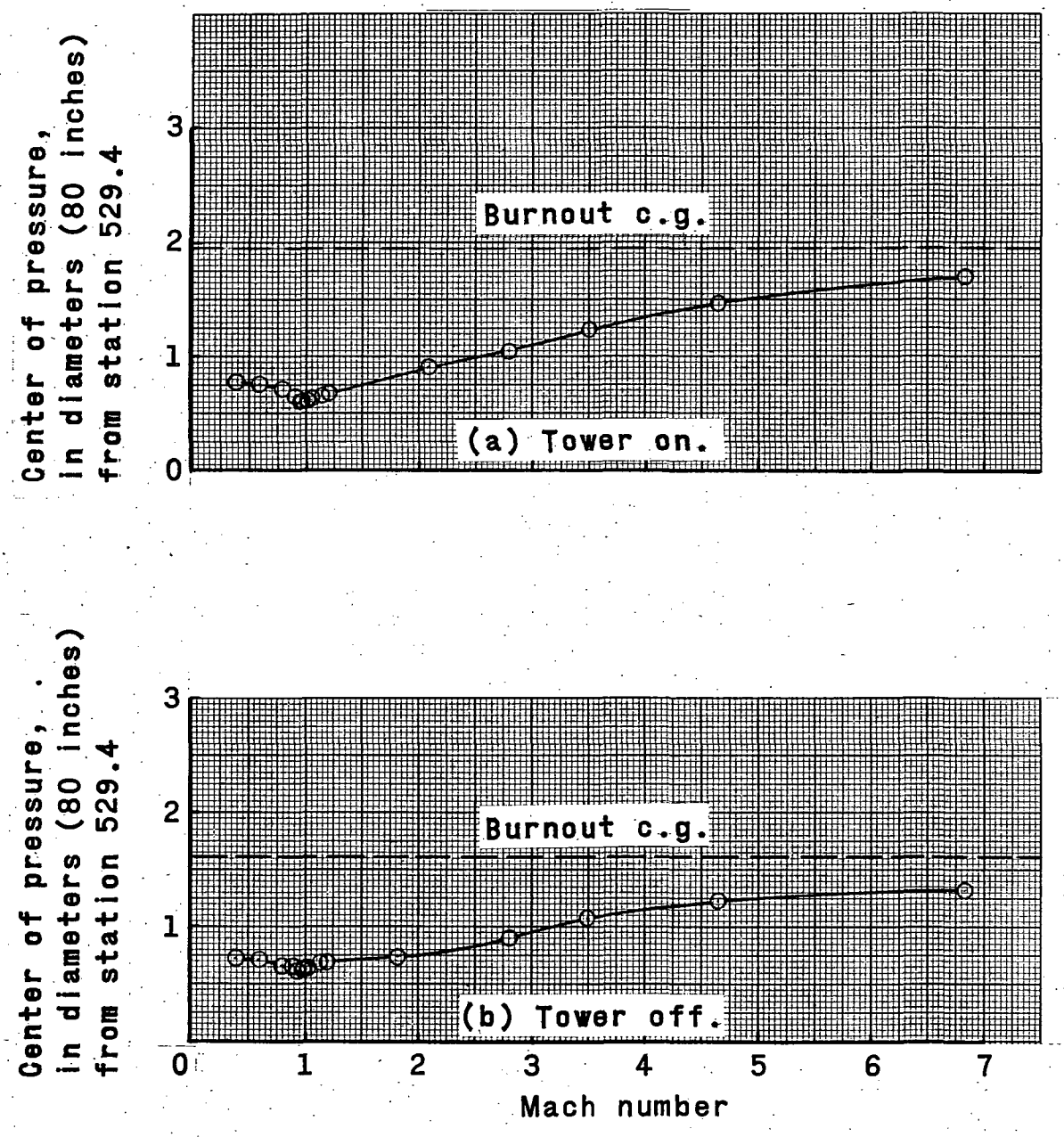

Figure 7.- Variation of center of pressure in relation to Mach number for Little Joe vehicle.

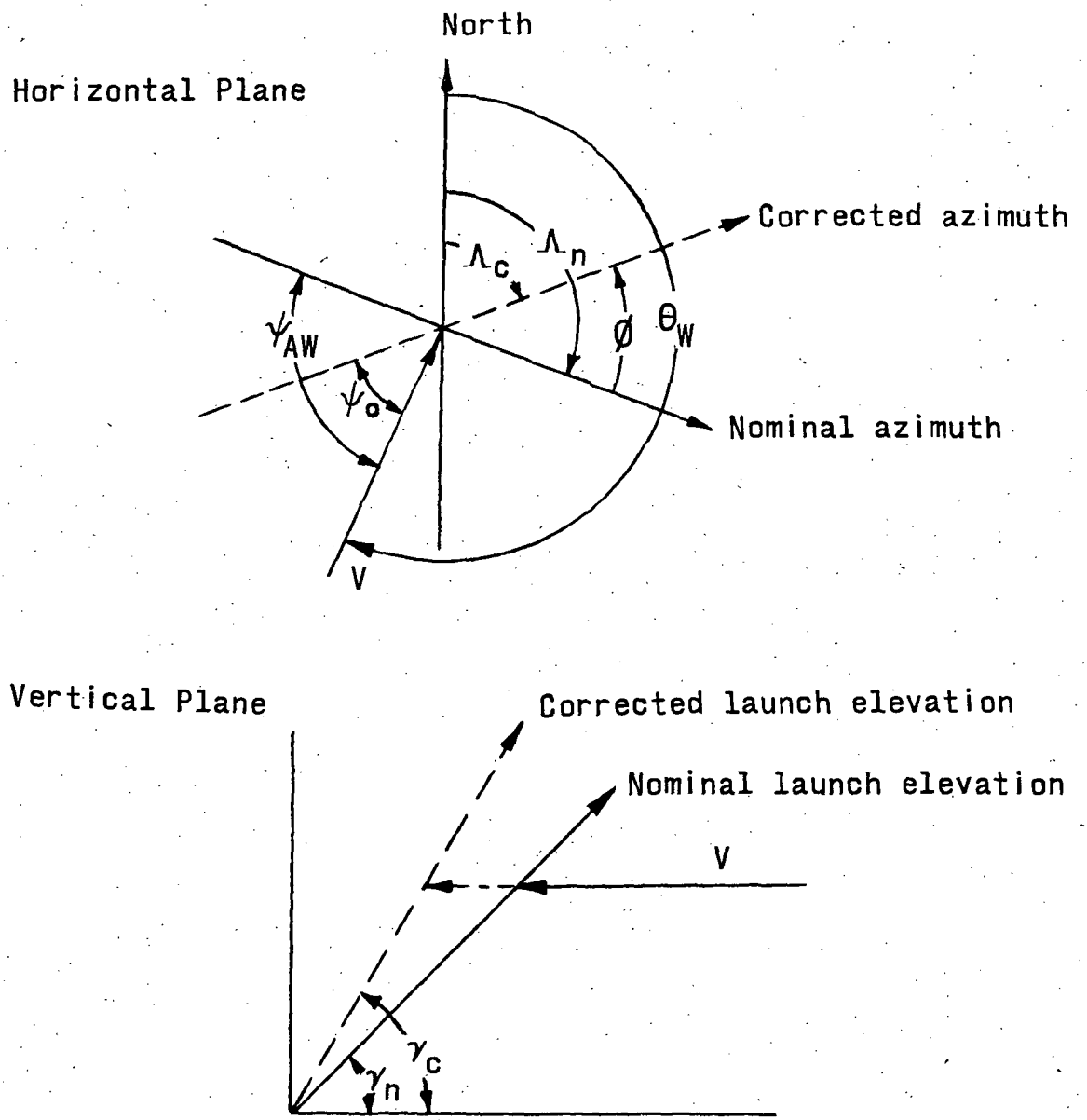

Figure 8.- Angles associated with rocket vehicle.

G-4

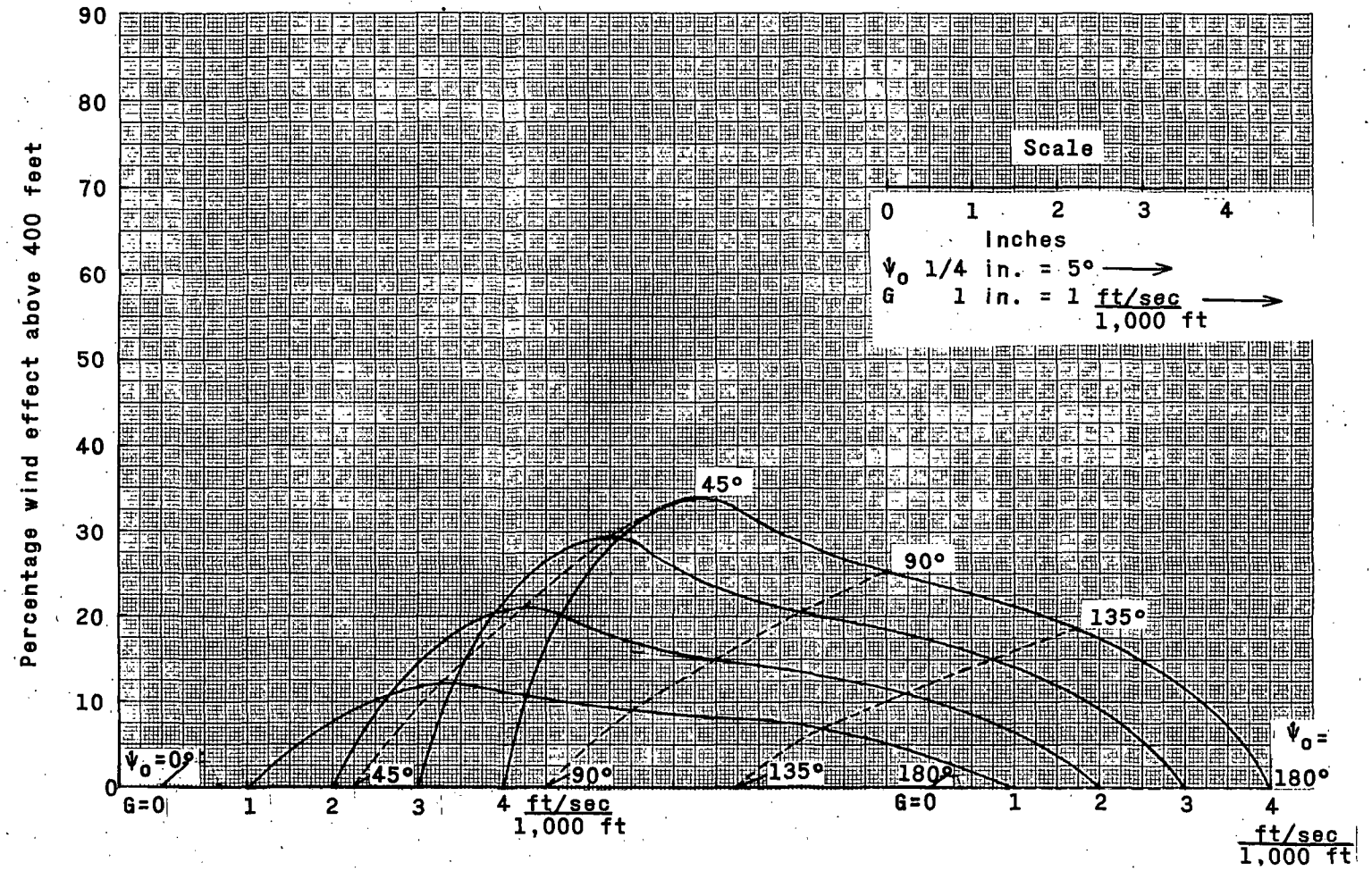

Figure 9.- Percentage wind effect on heading angle of typical Little Joe vehicle above 400 feet altitude.

CONFIDENTIAL

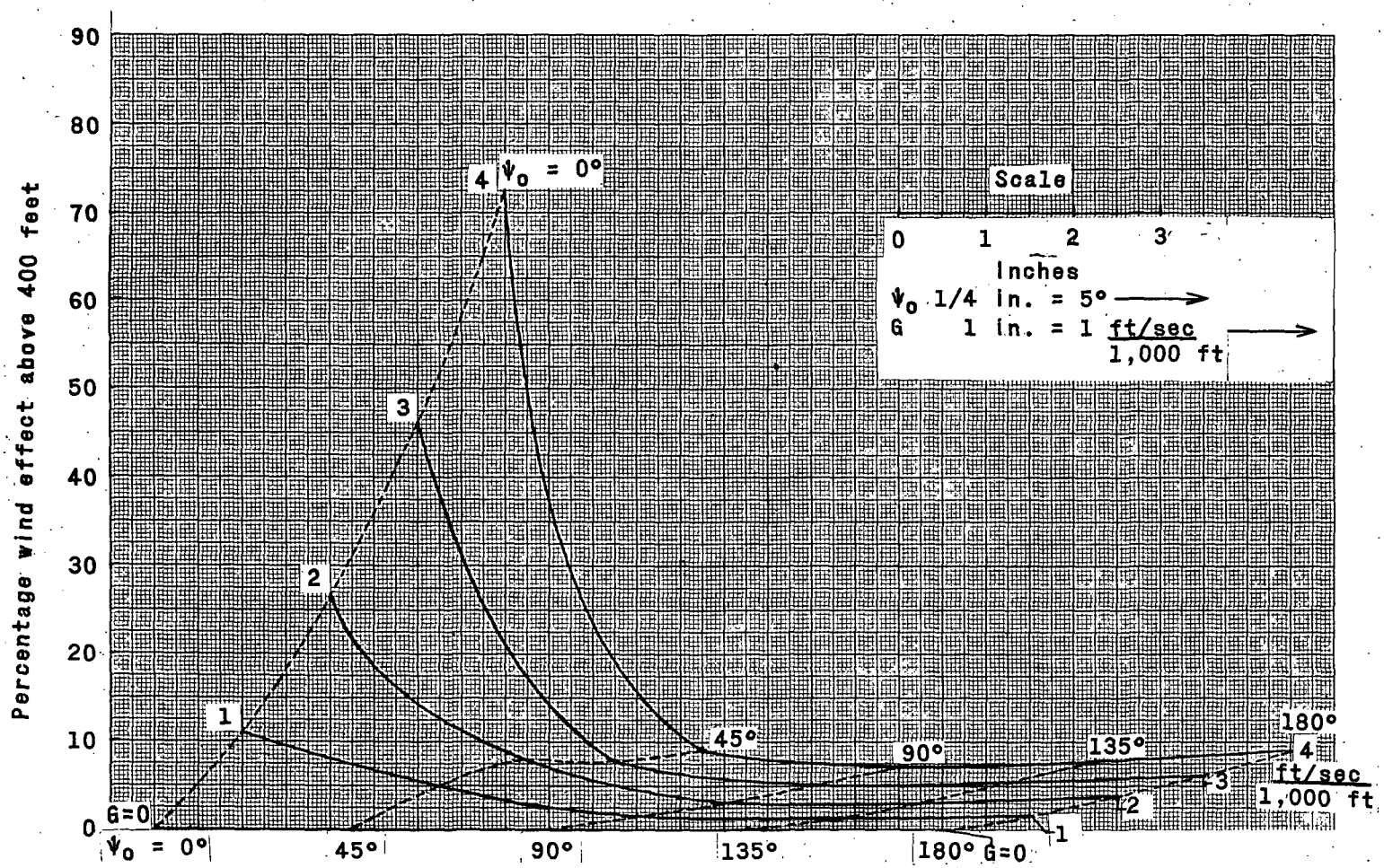

Figure 10.- Percentage wind effect on flight-path angle of typical Little Joe vehicle above 400 feet altitude.

CONFIDENTIAL

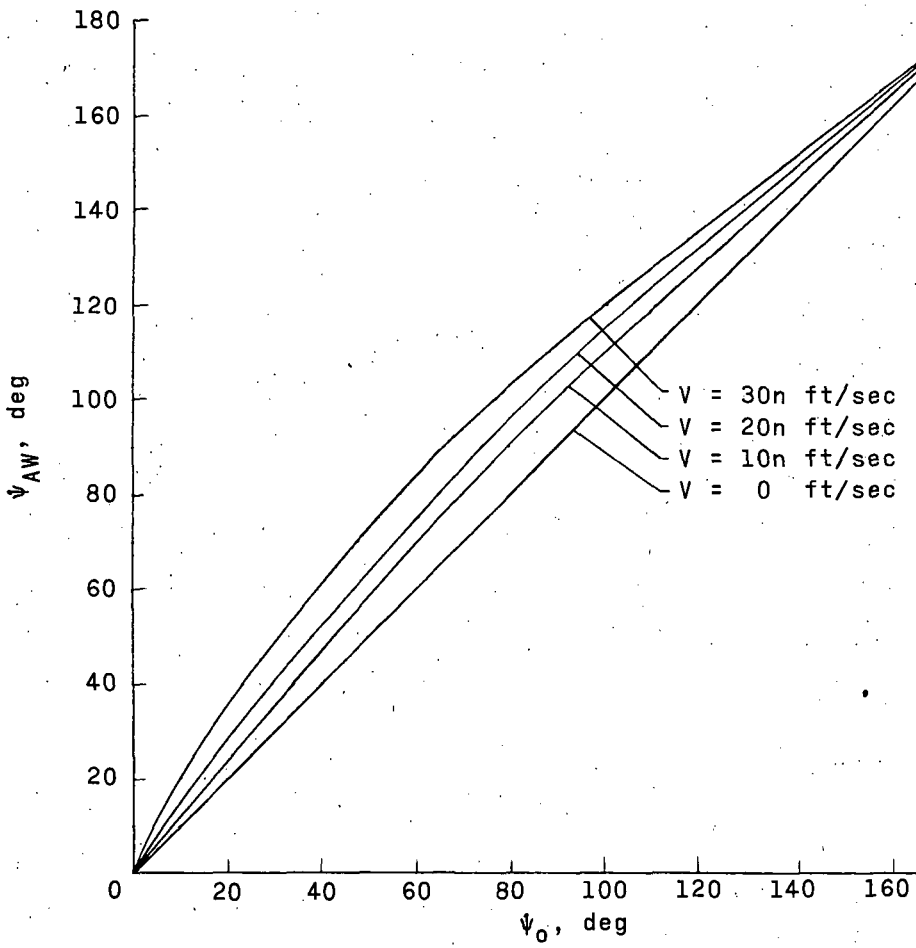

Constructing the plot in order to determine ψ_{AW}

V = 10n ft/sec

ψ_o	+ $\Delta\psi$	= ψ_{AW}
20	4	24
45	8	53
90	10	100
120	8	128
180	0	180

V = 30n ft/sec

ψ	+ $\Delta\psi$	= ψ_{AW}
20	15	35
45	22	67
90	21	111
120	15	135
180	0	180

Reading the plot to determine ø to be applied to the desired azimuth angle.

V = 10n ft/sec

ψ_{AW}	- ψ_o	= ø
20	17	3
45	38	7
90	80	10
120	111	9
180	180	0

V = 30n ft/sec

ψ_{AW}	- ψ_o	= ø
20	10	10
45	27	18
90	66	24
120	101	19
180	180	0

CONFIDENTIAL

Figure 11.- Final and initial angle of wind direction with respect to Little Joe type of vehicle subjected to different constant wind-velocity profiles. $\gamma = (m+5)^o$.

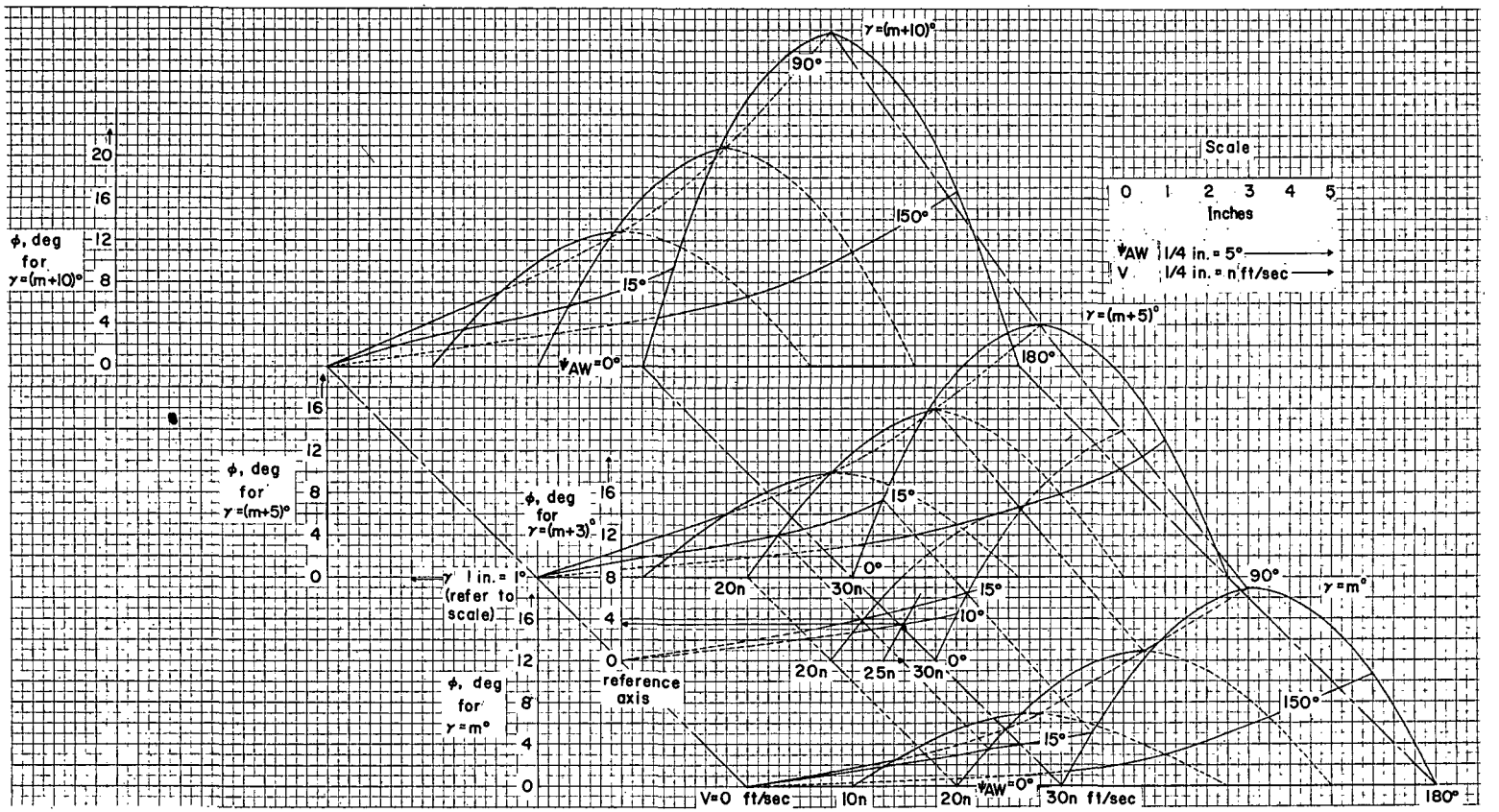

Figure 12.- Carpet plot giving azimuth correction angles compensating for wind effects on nominal launcher setting of typical Little Joe vehicle.

CONFIDENTIAL

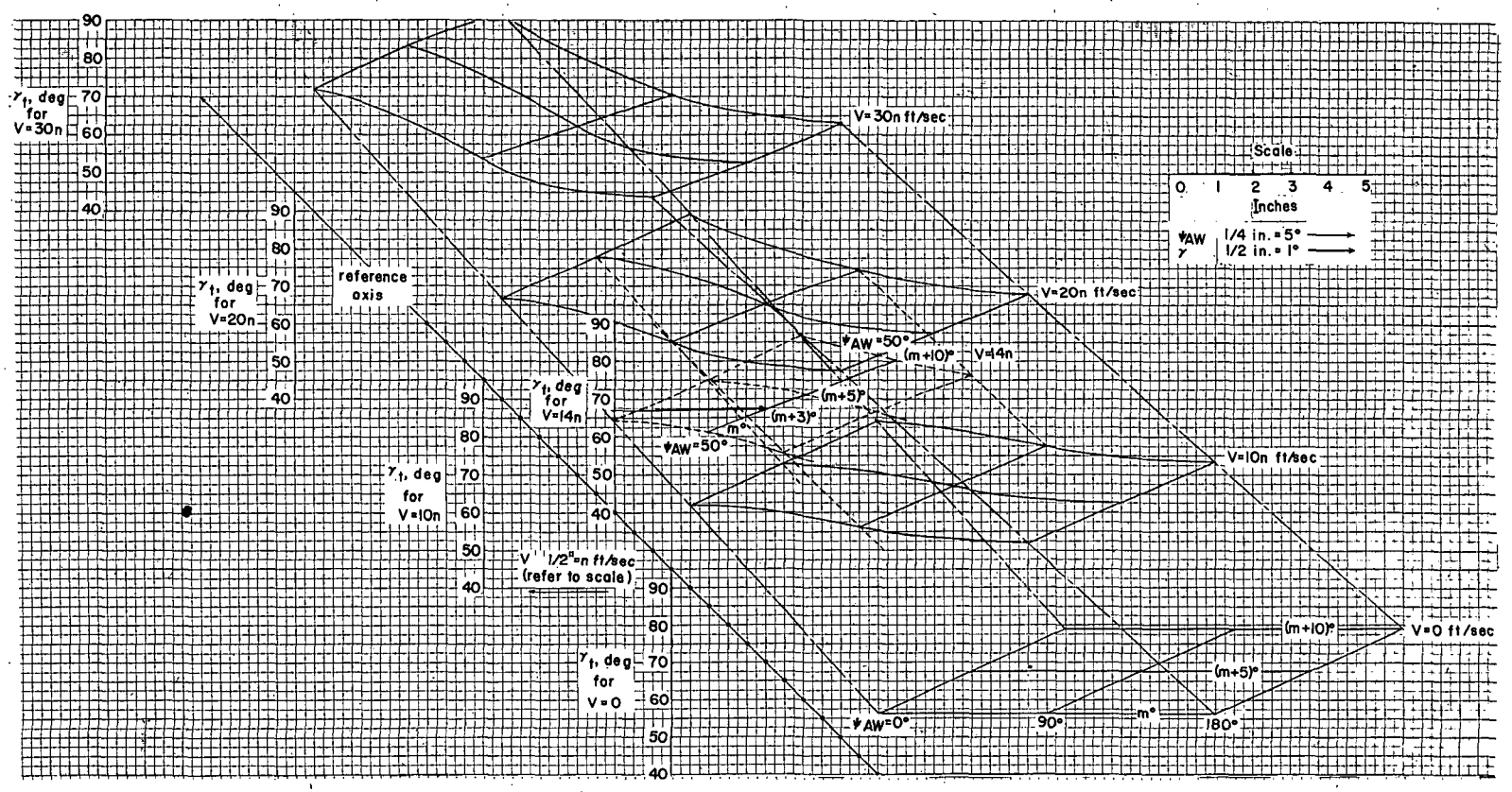

Figure 13.- Carpet plot yielding corrected elevation settings at launch compensating for wind effects on nominal launcher setting of typical Little Joe vehicle.

CONFIDENTIAL

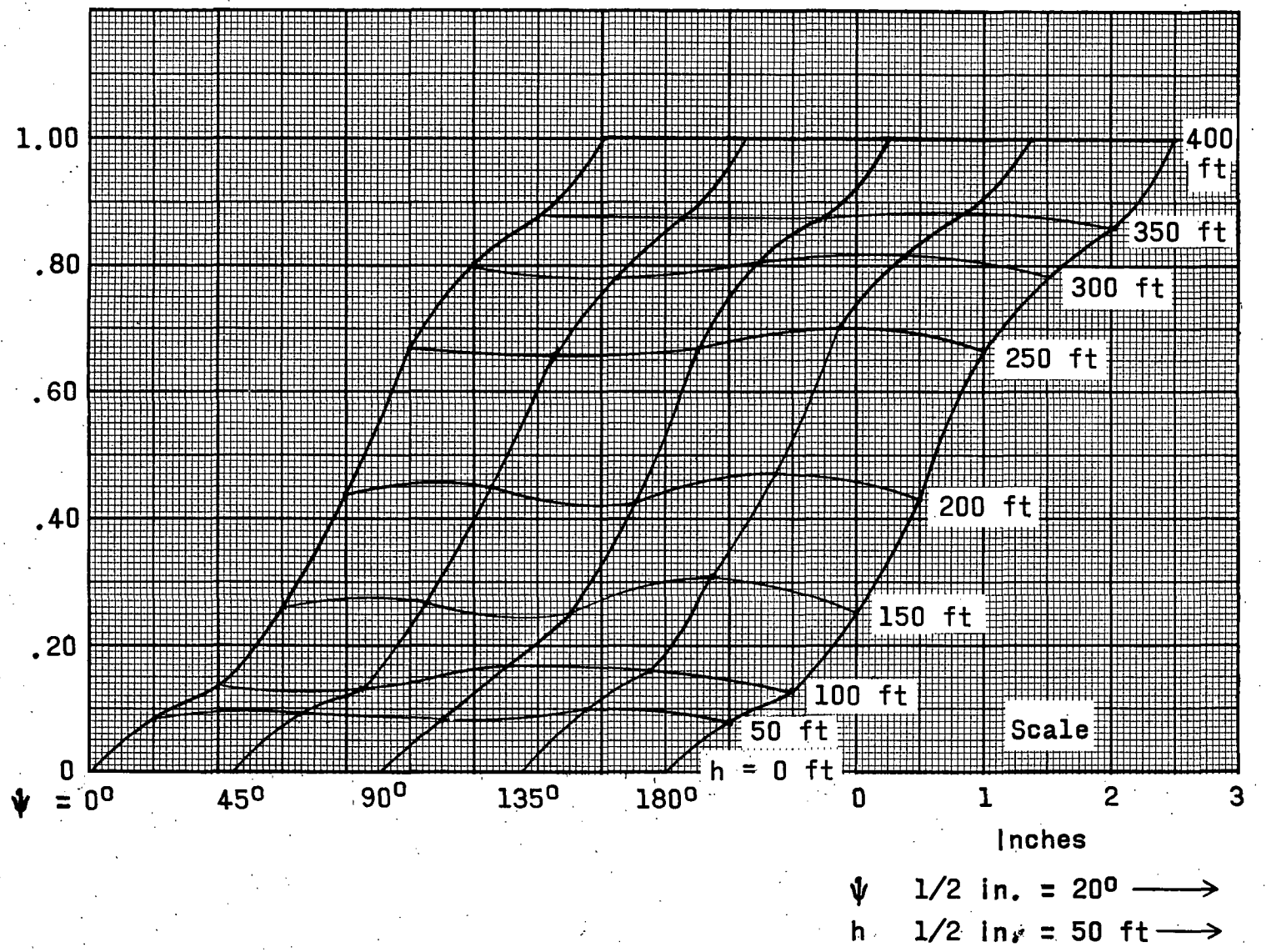

Figure 14.- Carpet plot showing weighting factors for wind velocity in relation to altitude and angle of wind direction with respect to typical Little Joe vehicle.

CONFIDENTIAL

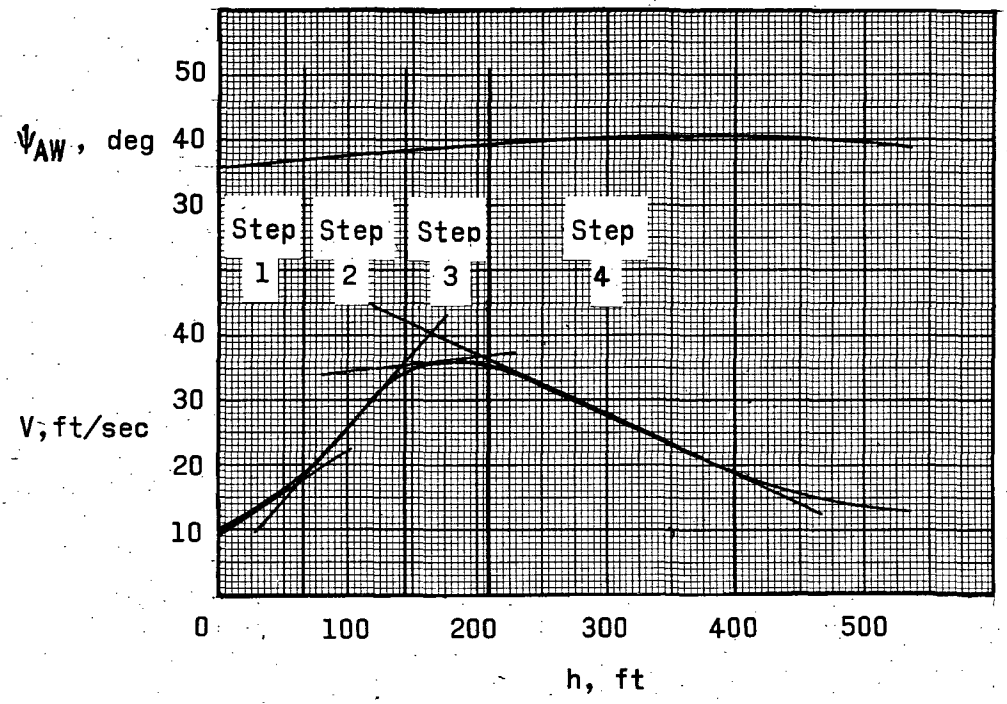

	$\bar{V}$	$\bar{\Psi}_{AW}$	WF	WF x $\bar{V}$	WF x $\bar{V}$ x cos $\bar{\Psi}_{AW}$	WF x V x sin $\bar{\Psi}_{AW}$
Step 1	14	36.5	0.12	1.68	1.36	0.99
Step 2	27	37.5	.16	4.33	3.44	2.65
Step 3	36	39.0	.20	7.20	5.61	4.54
Step 4	28	40.0	.52	14.60	11.20	9.40
					Σ = 21.61	17.58

Find the resultant vector

Average weighted wind velocity, 27.8 ft/sec

Average weighted angle of wind direction with respect to the vehicle, 39°

Figure 15.- Example of wind-weighting procedure.

DECLASSIFIED

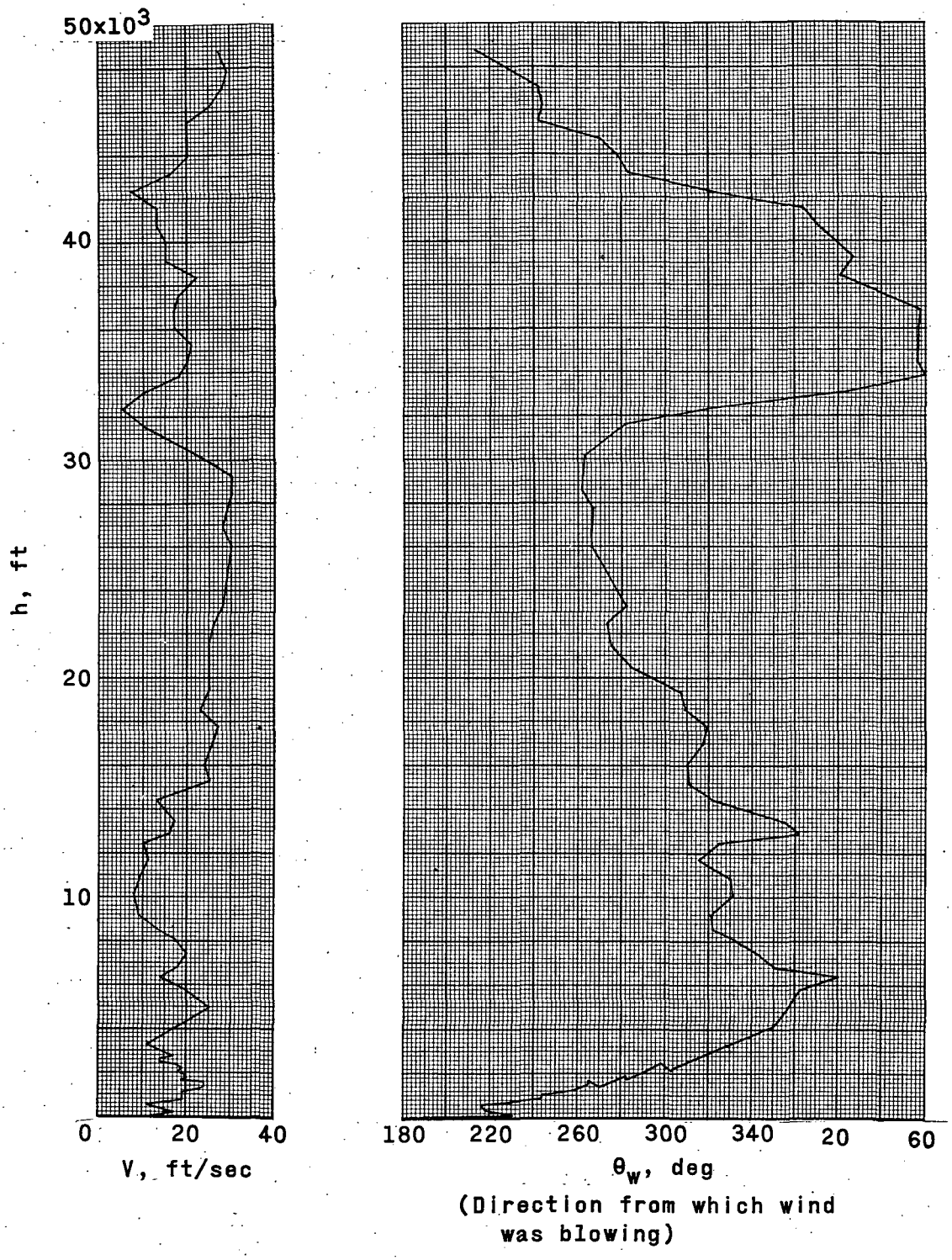

Figure 16.- High-altitude wind profile measured on day of first Little Joe flight test.

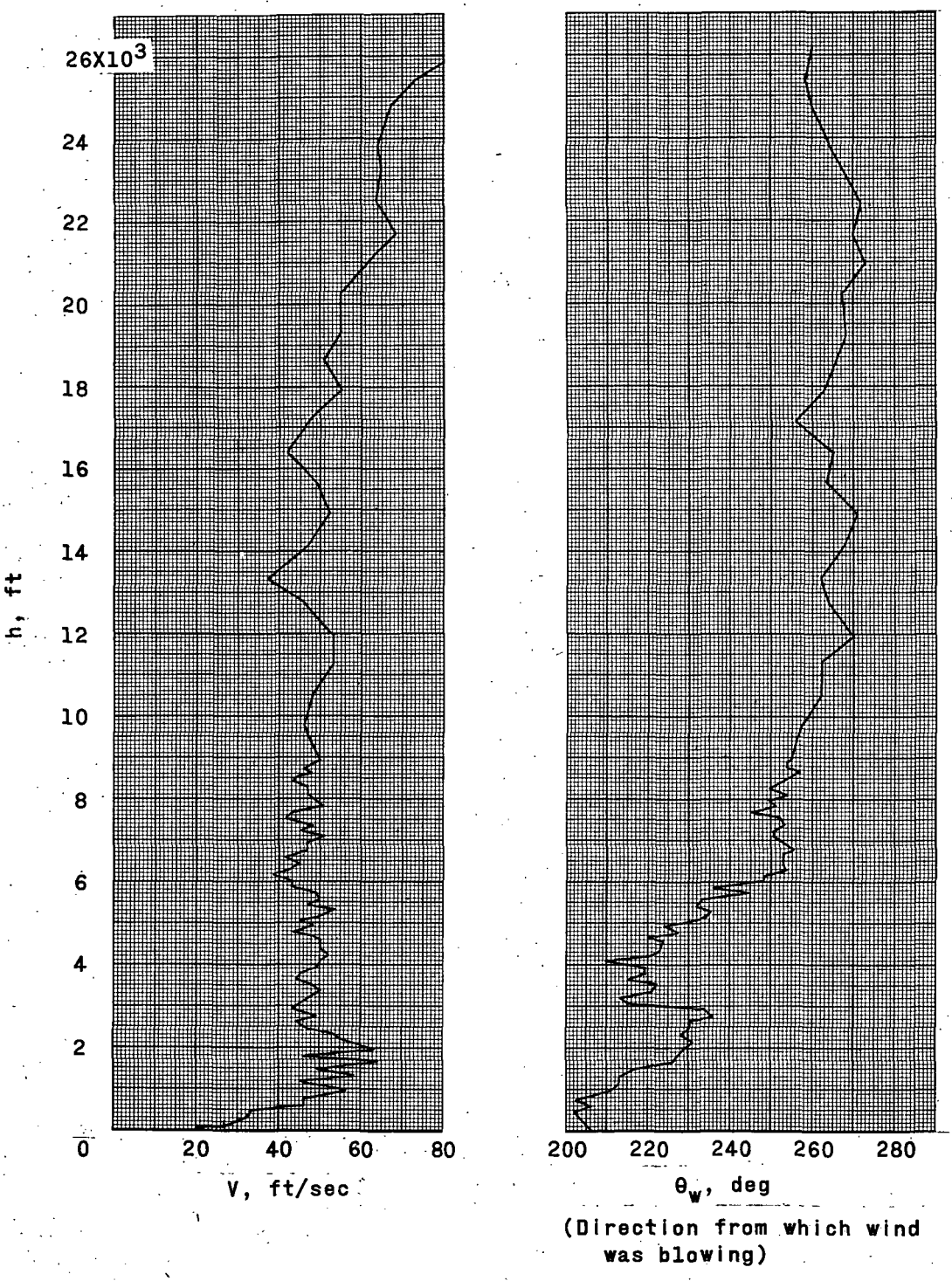

Figure 17.- High-altitude wind profile measured on day of second Little Joe flight test.

DECLASSIFIED
CONFIDENTIAL

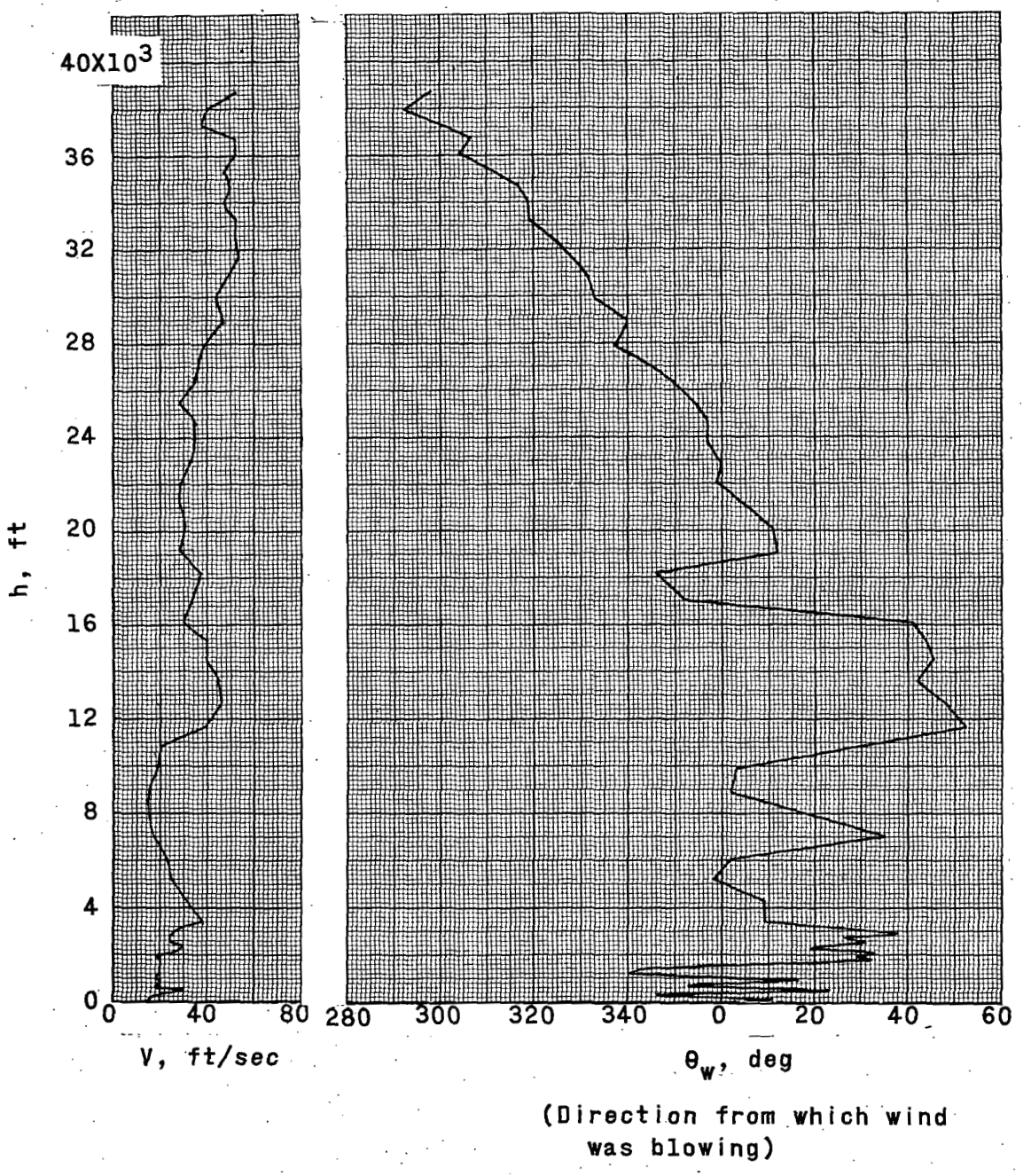

Figure 18.- High-altitude wind profile measured on day of third Little Joe flight test.

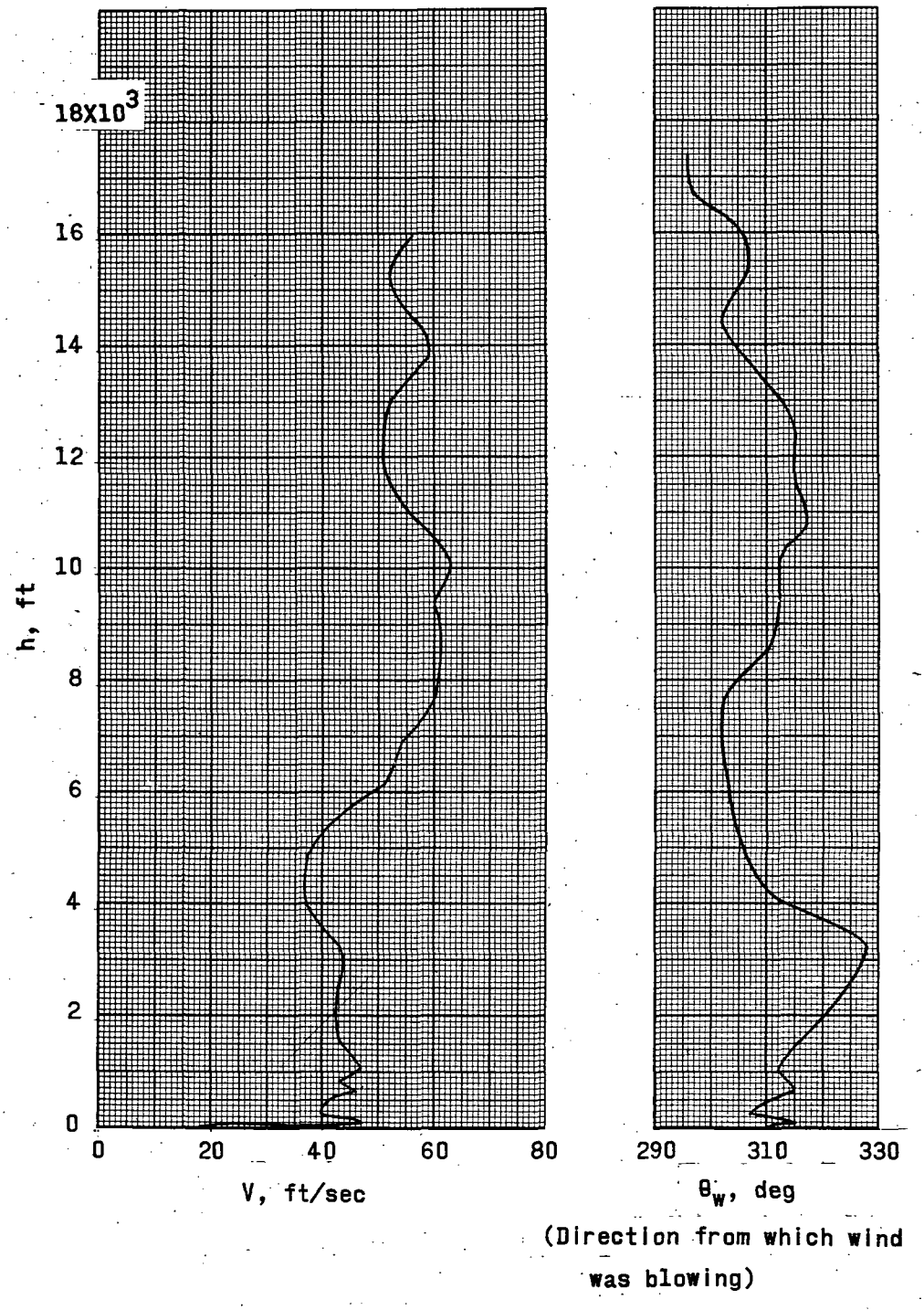

Figure 19.- High-altitude wind profile measured on day of fourth Little Joe flight test.